Summer 8-21-2022

Characterization of a Stenotrophomonas maltophilia Bacteriophage

Edward Eshoo
DePaul University, EESHOO@depaul.edu

Characterization of a *Stenotrophomonas maltophilia* Bacteriophage

By

Edward Eshoo

Department of Biological Sciences

College of Science and Health

DePaul University, Chicago, Illinois

Acknowledgements

I would like to thank the members of my thesis committee (Dr. Joanna Brooke, Dr. Megan Schrementi, and Dr. Timothy Sparkes) for their guidance and support throughout my tenure at DePaul University. First, I would like to give a special thank you to my thesis advisor, Dr. Brooke, for her guidance, support, and training. For the career path that I am currently on, there is not a better advisor that I could have chosen. Her expertise in the field, and wisdom from a lifetime of scientific research, has been the example that I have tried to emulate in my own work. I would not have become the scientist that I am today without her constantly challenging me to improve and the encouragement she provided when my confidence wavered. Her commitment to our research, and dedication to seeing this project through, have meant more to me than I can put into words. I have come a long way since the start of this program and she has stuck with me all these years, through the ups and downs, and for that I cannot thank her enough.

I would also like to thank Dr. Schrementi for the mentorship and support that she provided over these past few years. During my time in the program, Dr. Schrementi has given me invaluable instruction on the technical skills required for research in microbiology. From basic techniques to the advanced, what I have learned from her will stay with me throughout the rest of my scientific career. Her ability to encourage me when necessary, and to challenge me when essential, has been instrumental to my growth both in the laboratory and classroom. Through her example, I have improved my presentation and teaching skills to a level that might not have seemed possible at the beginning of this program. Under Dr. Schrementi's guidance, I have developed into a capable and respected teaching assistant, something that I could not have been done without her.

I would like to thank Dr. Sparkes for his encouragement and guidance as both a mentor and role model. Even as the Chair of the department, he has always made himself available to help Dr. Brooke and I with this thesis project, including experimental design and statistical analysis. My development as a graduate student would not have been possible without people like Dr. Sparkes to push me forward and keep me on track. With his help, I have reached a level of knowledge and confidence that hardly resembles the man that walked into his Intro to Graduate Studies course on the first day of this program.

I also want to thank Rima Barkauskas for the role that she played in the development of my research and teaching abilities. Across several courses, her guidance and insight have allowed me to refine my skills in oral presentation and the management of my responsibilities as a teaching assistant. The skills and techniques that I learned under Rima have been translated into my own research, and have allowed us to expand this thesis project beyond what we initially envisioned. Without Rima, I don't think I could have cultivated the attributes to be in the position that I am today.

In addition to the aforementioned faculty members, I would like to thank my lab members, Lydia Walther, Sophia Zygowski, and Hilvin Molina for their support and assistance with many aspects of this project. I could not have done this alone and I am lucky that I have had the chance to work with them to put a complete thesis in front of my committee and the department. Specifically, Lydia and Sophia were instrumental to the latter half of this thesis research. We worked closely to complete temperature and pH stability experiments, SDS-PAGE, and adsorption assays. Even though my time in the lab is over, I only hope that I can help them as much as they have me.

We would also like to thank Dr. Dave Rademacher and Loyola University for the imaging of our bacteriophage. Dr. Rademacher was very gracious with his time and arranged his schedule to meet with us on several occasions, all of which resulted in fantastic images of our isolated bacteriophage. Our lab looks forward to working with Dr. Rademacher again in the future.

Lastly, but definitely not least, I would like to give a special thank you to the friends and family that have made this graduate experience worthwhile. To my parents, your unconditional love and support has been the driving force behind my achievements and has inspired the success of my scientific career. I cannot thank you enough for believing in me, even when others might not have. I would not be the person that I am today without the strength of your foundation behind me. The acknowledgements section is still short to tell you both how much you mean to me but it is certain that I would not have gotten this far without you. To my sister, thank you for believing in me and trusting that I would come out on top when it really mattered. You always knew that somehow, someway, I could do it, and your support has given me strength even when I could not find it elsewhere. To my grandparents, you have watched the years go by, you have seen me grow and change, and I only hope that you are proud of the person that I am now. Your unbridled love and support has meant the world to me and you have remained my biggest fans until the very end. My journey will not end here and I look forward to you reading the next chapter. Thank you everyone, for everything.

Abstract

Stenotrophomonas maltophilia is a ubiquitous Gram-negative, multidrug resistant, opportunistic bacterial pathogen that causes various infections in humans. Recently, the use of bacteriophages as therapeutic agents, has gained interest as an alternative to traditional antibiotics. This thesis describes the isolation, purification, and characterization of *S. maltophilia* bacteriophage Bfi2 and discusses its activity against related, and often co-isolated, bacterial pathogens. Amplification of the phage resulted in clear, well-defined plaques and a titer of $1.73 \pm 0.38 \times 10^{11}$ PFU/ml. Bfi2 demonstrated the ability to lyse 55% of the *S. maltophilia* strains tested, suggesting that it has a moderate host range. However, the phage did not show cross taxonomic order infectivity, as the other bacterial species tested were not susceptible to infection. Efficiency of plating (EOP) assays shown Bfi2 to be nearly half as effective against another susceptible strain of *S. maltophilia*, F7221, compared to the host strain. Digestion of Bfi2 nucleic acid by type II restriction endonucleases, and visualization of products by agarose gel electrophoresis, indicated that the phage contained a dsDNA genome with an estimated size of 66.5 kb. Electron microscopy determined that Bfi2 has an icosahedral capsid 75.3 ± 3.3 nm by 69.6 ± 3.9 nm and a flexible, non-contractile tail 154.2 ± 4.6 nm by 9.3 ± 0.5 nm. Together, electron microscopy and genomic analysis suggests that Bfi2 likely belongs to the family *Siphoviridae*, with a B1 morphotype. Bfi2 was found to be stable at a temperature of 30°C. However, Bfi2 became increasingly unstable at 50°C over time, and quickly lost activity at 60°C. Moreover, Bfi2 was found to be stable at pH 5, 7, and 9. The kinetics of Bfi2 adsorption to host cells were determined. Bfi2 was found to have a relatively high adsorption efficiency, where ~97% of phages were adsorbed to host cells after 15 minutes of incubation. The adsorption rate constant (k) of Bfi2 was calculated to be $\sim 2.15 \pm 0.06 \times 10^{-9}$ ml min^{-1} at a multiplicity of infection (MOI) of 0.05. Bfi2 may be suitable for future therapeutic applications based on its lytic activity and moderate host range.

Table of Contents

I. Introduction

Due to increasing concerns over antibiotic resistance, the use of bacteriophages (phages), viruses that infect bacteria, is being examined as a promising alternative strategy for the treatment of multi-drug resistant (MDR) bacterial pathogens. In the past few decades, there have been renewed interests in the therapeutic applications of phages. Exploration into the application of phages in Western countries slowed soon after the introduction of antibiotics. However, several Eastern European countries have continued to make advancements in this field. Institutions within these countries have provided personalized phage therapy to patients with chronic antibiotic-resistant infections that have not been responsive to traditional regimens (Chanishvili, 2012, 2016; Górski et al., 2018; Häusler, 2006; Kutateladze, 2015; Kutateladze and Adamia, 2008, 2016).

Gram-negative bacterial pathogens are of clinical interest, often possessing high levels of antibiotic resistance due to inherent structural or functional characteristics (Kidd et al., 2018). Gram-negative pathogens, such as *Stenotrophomonas maltophilia*, often display several acquired and intrinsic mechanisms of antibiotic resistance (Alonso and Martinez, 1997; Barbolla et al., 2004; Brooke, 2012; Sánchez, 2015). This bacterium has emerged as an important global and nosocomial (hospital-acquired) pathogen, particularly for the immunocompromised, and its frequency of isolation is increasing (Brooke, 2012; Sanyal and Mokaddas, 1999). Consequently, the treatment of *S. maltophilia* infections is thwarted by this bacterium's resistance to most drugs, which has forced clinicians to pursue novel and effective treatment strategies.

Despite growing support from primary scientific research and early phase clinical trials, phage therapy is struggling to develop in Western countries (Brives and Pourraz, 2020). Compared to antibiotics, phages possess a fundamentally different mode of antimicrobial activity, where they have shown the ability to bypass bacterial cell walls and the extracellular matrix of biofilms en

route to infection of the host (Chang et al., 2019; Forti et al., 2018; Loessner, 2005; Waters et al., 2017). To date, only a limited number of phages with activity against *S. maltophilia* have been reported and characterized for their therapeutic potential (McCutcheon and Dennis, 2021; Peters et al., 2020). If phage therapy is to become a valuable alternative for the treatment of drug-resistant bacterial pathogens, particularly *S. maltophilia,* more research is required to expand the collection of documented phages and to fully characterize their biological activity both *in vitro* and *in vivo*.

It was hypothesized that a phage with activity against *S. maltophilia* could be isolated from the environment and that its biological properties can be characterized *in vitro.* This thesis research describes the isolation of a *S. maltophilia* bacteriophage, characterizes its biological properties *in vitro*, and discusses its activity against *S. maltophilia* strains and related and co-isolated bacterial pathogens. The bacteriophage was isolated from soil samples through conventional enrichment techniques and double-layer plaque assays (Gill and Hyman, 2010; Hyman, 2019; Hyman and Abedon, 2009). Transmission electron microscopy (TEM) and ultrastructure measurements suggests the isolated phage belongs to the family *Siphoviridae*, with a B1 morphotype. Phage host range and relative lytic efficiency were determined through conventional spot tests and efficiency of plating (EOP) assays. Nucleic acid isolation and analysis provided valuable information on the composition and size of the phage genome. Moreover, phage structural stability in response to pH and temperature was assessed. Additional characterization of phage growth kinetics, including adsorption efficiency and adsorption rate constant (k), were determined. This study concludes that the isolated phage may be a suitable candidate for therapeutic applications against *S. maltophilia* due to desirable traits such as its lytic nature and moderate host range. However, further investigation into its genome content, stability, anti-biofilm activity, in addition to efficacy and safety *in vivo* is necessary for the phage to be considered as a candidate for phage therapy.

Preliminary biofilm assays (data not shown) revealed that the isolated phage described in this thesis has the ability to inhibit biofilm formation of *S. maltophilia* strain K279a. For the purpose of discussion and comparison, the phage described herein will be referred to as Bfi2 (Biofilm formation inhibition 2), due to its anti-biofilm activity.

II. Literature Review

The Global Problem of Multi-drug Resistant Bacteria

The concern over multi-drug resistant (MDR) bacteria has become widespread and recently the World Health Organization (WHO) declared the issue of antimicrobial resistance a global crisis (Shrivastava et al., 2017). Reviews have attributed the rising rates of MDR infections as a consequence of several compounding factors including the prolonged use of antibiotic drugs, acquisition of resistance genes, and selection of 'hypermutator' strains (Kidd et al., 2013, 2018; Ng et al., 2020; Vidigal et al., 2014). Mechanisms of acquired resistance and a lack of rigid control measures (through the cross infection of MDR strains) have allowed these bacteria to effectively become pan-resistant to all currently available antibiotic drugs (Crossman et al., 2008; Fothergill et al., 2012; Johansen et al., 2008; Mesaros et al., 2007; Ng et al., 2020; Parkins et al., 2014; Salunkhe et al., 2005).

Several limitations, including the development of drug allergy and toxicity, still confront the long-term use of antimicrobial drugs for the treatment of MDR infections (Gao et al., 2017; Kalghatgi et al., 2013; Levison and Levison, 2009). These limitations, coupled with the emergence of MDR pathogens, are often correlated with lengthier hospitalizations and higher rates of re-admittance (Ng et al., 2020). The detriments of long-term antibiotic regimes make the treatment of chronic MDR bacterial infections especially difficult for aging and immunocompromised populations (DeNegre et al., 2019).

S. maltophilia is an Opportunistic Pathogen

S. maltophilia is an aerobic, non-fermenting, Gram-negative bacterium (Brooke, 2012). It is ubiquitous in nature and has emerged as a concerning opportunistic pathogen due to its profile of multi-drug resistance (Brooke, 2012). Exposure of *S. maltophilia* to humans can occur both in and outside clinical settings (Brooke, 2012). In clinical settings, MDR isolates of *S. maltophilia* have been recovered from several sources including, hemodialysate, tap water, and treated water samples (Arvanitdou et al., 2003; Brooke, 2012).

This pathogen's tolerance and inherent broad resistance to antibacterial drugs, including most, if not all, β-lactams, have allowed it to become an important opportunistic pathogen (Brooke, 2012; Denton and Kerr, 1998). As a result, *S. maltophilia's* incidence in the cause of bacteremia (infections of the bloodstream) by Gram-negative bacteria is second only to that of *Pseudomonas aeruginosa* (Gales et al., 2006; Jones et al., 2003; Sader and Jones et al., 2005; Sanyal and Mokaddas, 1999). Like that of *P. aeruginosa*, *S. maltophilia* has been identified as a significant pathogen in the immunocompromised population (Baumrin et al., 2017; Brooke, 2012; Kim et al., 2019). Particularly, *S. maltophilia* has been isolated from individuals suffering from cystic fibrosis (CF) and is estimated to infect 10-18% of CF patients in Western countries such as Australia, Canada, and the United States (Parkins and Floto, 2015; Salsgiver, et al., 2016).

Infections associated with *S. maltophilia*

It is important to note that *S. maltophilia* is not solely a nosocomial pathogen (Brooke, 2012). The variety of *S. maltophilia* infections in humans include but are not limited to: bacteremia (Jang et al., 1992; Lai et al., 2004, 2006; Papedakis et al., 1995; Victor et al., 1994), biliary sepsis (infection of the organs and ducts that produce and store bile) (Papedakis et al., 1995), catheter-related bacteremia (Lia et al, 2006), cellulitis (infection of the skin) (Downhour et al., 2002),

chronic obstructive pulmonary disease (COPD) (Ewig et al., 2000; Nseir et al., 2006), endophthalmitis/keratitis (Akcakaya et al., 2011; Chen et al., 2010), meningitis (Nguyen and Nuder, 1994), pneumonia (Ewig et al., 2000; Fujita, 1996; Sefcick et al., 1999), osteomyelitis (Landrum et al., 2005), urinary tract infections (Vartivarian et al., 1994), as well as other infections of the skin and soft tissues (Bin Abdulhak et al., 2009; Sakhnini et al., 2002).

Reports have identified *S. maltophilia* as being associated with community-acquired (CA) infections (Brooke, 2012). CA infections for both children and adults include bacteremia, ocular infections, respiratory tract infections, and cellulitis (Falagas et al., 2009). There has been a notable rise in community-acquired *S. maltophilia* infections; this may mirror the overall trend of increasing CA opportunistic infections by MDR bacteria (Brooke, 2012; Falagas et al., 2009).

Antibiotic Treatment of *S. maltophilia*

Currently, trimethoprim-sulfamethoxazole (TMP-SMX) is the recommended antibiotic for *S. maltophilia* infections (Chang et al., 2015). However, resistance rates of *S. maltophilia* to TMP-SMX have been reported to be higher in patients with cancer and CF, highlighting the concern over the emergence of resistance within the immunocompromised community (Al-Jasser, 2006; Canton et al., 2003; Micozzi et al., 2000; Saiman et al., 2002; San Gabriel et al., 2004; Valenza et al., 2008; Vartivarian et al., 1994). Though surveillance studies of TMP-SMX are few, the geographic distribution of higher rates of TMP-SMX resistance in *S. maltophilia* suggests that resistance to this drug is increasing worldwide (del Toro et al., 2002; Flores-Treviño et al., 2014; Gülmez and Hascelik 2005; Hotta et al., 2014; Lai et al., 2004; Memish et al., 2012; Rattanaumpawan et al., 2013; Rhee et al., 2013; Valdezate et al., 2001; Walkty et al., 2014; Wang et al., 2014; Wu et al., 2012; Zhanel et al., 2013). The occurrence of medical contradictions, toxicity, and the emergence of resistance to these drugs in *S. maltophilia* has reignited investigation

into the development of novel alternative treatment strategies (Brooke, 2012, 2014; Ho and Juurlink, 2011).

Mechanisms of Antibiotic Resistance in *S. maltophilia*

The emergence of multi-drug resistance in *S. maltophilia* is not solely a consequence of antibiotic misuse. This bacterium possesses both innate and acquired resistance mechanisms, including chromosomally encoded β-lactamases, aminoglycoside-modifying enzymes, multi-drug efflux pumps, and the presence of mobile genetic elements (MGE) (Alonso and Martinez, 1997; Barbolla et al. 2004; Breijyeh et al., 2020; Chung et al., 2015; Huang et al., 2015; Lin et al., 2014, 2015; Ruppé et al., 2015; Sanchez, 2015). These MGEs include plasmids, transposons, and autonomously integrating gene cassettes termed integrons (Chung et al., 2015; Domingues et al., 2012; Hall and Collis, 1995; Hu et al., 2011; Sköld et al., 2001; Toleman et al., 2006, 2007). Strains of *S. maltophilia* have been reported as resistant to all known β-lactams, aminoglycosides, quinolones, tetracyclines, as well as chloramphenicol, rifampin, and TMP-SMX (Al-Jasser, 2006; Alonso and Martinez, 1997; Traub et al., 1998). The major antibiotic resistance mechanisms identified in *S. maltophilia* are presented in Table 1.

Mechanism	Type	Conferred Resistance	Reference
β-lactamases	L1, L2	β-lactams	(Huang et al., 2010; Okazaki and Avison, 2008)
Efflux pumps	ABC, MFS, RND, Fusaric acid	Aminoglycosides, β-lactams, chloramphenicol, macrolides, quinolones, sulfonamides, tetracyclines, and TMP-SMX	(Alonso and Martinez, 2000; Alonso et al., 2000; Chang et al., 2004; Chang et al., 2015; Lin et al., 2014, 2015)
Aminoglycoside-modifying enzymes	Aminoglycoside phosphotransferase, aminoglycoside N-acetyltransferase	Aminoglycosides	(Li et al., 2003; Okazaki and Avison, 2007)
Quinolone-resistance protein	SmQnr	Quinolones	(Chang et al., 2011; García-León et al., 2014, 2015; Sánchez and Martinez, 2010)
Mobile Genetic Elements	Integrons, ISCR, Plasmids, Transposons	TMP-SMX	(Chung et al., 2015; Huang et al., 2015; Hu et al., 2011; Sköld, 2001; Toleman et al., 2006, 2007)

Table 1: Major Mechanisms of Antibiotic Resistance in *S. maltophilia*.

Biofilms of *S. maltophilia*

In addition to the mechanisms of acquired resistance, *S. maltophilia* is recognized for its innate ability to form biofilms on both abiotic and biotic surfaces (Brooke, 2012; Vidigal et al., 2014; Steinmann et al., 2018; Pompilio et al, 2010). A bacterial biofilm is defined as an assemblage of bacterial cells that are irreversibly adhered to a surface and enclosed within a matrix composed of extracellular polymeric substances (EPS) (Donlan, 2002) (Figure 1). This EPS matrix predominantly consists of polysaccharides; but is also known to associate with DNA, lipids, or proteins, and is the main structural component of the biofilm (Donlan, 2002; Flemming et al., 2000).

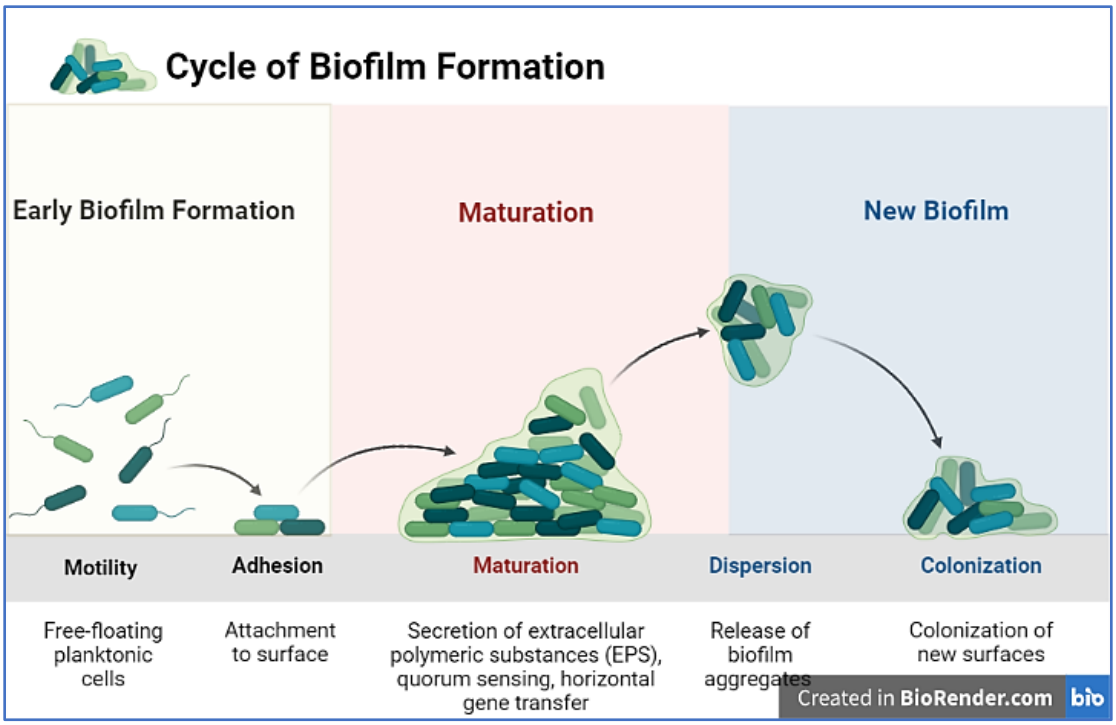

Figure 1: Steps of Biofilm Formation. Adapted from 'Biofilm template', BioRender (2022).

As depicted in Figure 1, biofilm formation occurs in sequential steps beginning with the adherence of bacterial cells to a solid surface (Figure 1, 'Adhesion'). Once adhered, aggregates of bacterial cells coordinate through quorum sensing (QS) (regulation of gene expression through the detection and response to cell population density) and begin to produce EPS (Figure 1, 'Adhesion-

Maturation') (Donlan, 2002). Cells enclosed within the EPS matrix continue to share resources and divide until biofilm maturation is complete (Figure 1, 'Maturation'). Upon maturation, cells within the biofilm may be dispersed, where they have the potential to colonize new surfaces (Figure 1, 'Dispersion-Colonization').

Biofilms are important microbial structures that enable the establishment of persistent infections (Donlan, 2002). Once matured, the interior of a biofilm creates concentration gradients that provide optimal microhabitats, allows for the exchange of genes, and facilitates cell-cell communication (Stewart, 2003). Furthermore, biofilms may be dispersed by the shedding of actively dividing daughter cells, detachment as a result of QS, or by shearing of biofilm cells due to continuous flow effects (Donlan, 2002). Complete eradication of biofilms is difficult, as the dispersal of cells from the matrix can increase the persistence of an infection when aggregates of the biofilm travel to and colonize new areas (Donlan, 2002). The structure of biofilms, and their organization through QS, allow bacterial pathogens such as *S. maltophilia* to persist despite current and aggressive treatment regimens (Ferriol-González and Domingo-Calap, 2020; Solano et al., 2014). The biofilms and antibiotic resistance of *S. maltophilia* have necessitated the development or re-visiting of novel antibacterial strategies. Phage therapy, the clinical and selective use of bacteriophages to target and lyse specific bacterial cells, has experienced renewed interest.

Bacteriophages

Phages are self-replicating entities and their replication within bacterial hosts can quickly increase phage abundance at the site of the infection. After infection, phages appropriate the cellular machinery of their host to produce progeny virions, a process that ends with lysis of the bacterial cell (Principi et al., 2019; Young, 2013). The mechanisms used by phages to lyse host cells are effective against antibiotic-resistant bacteria, especially those that are Gram-negative.

Specifically, phages can bypass the structural defenses of host bacteria through the production of enzymes such as depolymerases (Fernandes and São-José, 2018; Knecht et al., 2020). These enzymes enable the breakdown of polysaccharides on the surface of bacterial cells. Therefore, depolymerase activity can make bacterial cell walls accessible for the injection of phage genomes into host cells during infection (Fernandes and São-José, 2018; Hyman, 2019; Jonge et al., 2019; Knecht et al., 2020).

The specific species or strains of bacteria that a bacteriophage can infect are considered to be within the phage's host range (Ross et al., 2016). Phages are limited to infecting a particular breadth of bacterial hosts that are often related or members of the same species (Hyman, 2019; Hyman and Abedon, 2009; Ross et al., 2016). The high specificity of phages towards their bacterial hosts is governed primarily by the interaction between phage receptor-binding proteins (RBPs) and bacterial cell surface receptors (Hyman, 2019; Jonge et al., 2019). The specific host range of phages enables a precise and targeted treatment strategy, without disruption of the patient's normal commensal and symbiotic microorganisms, even in the case of serotypes (distinct variants within a species of bacteria) (Lu and Breidt, 2015).

Bacteriophages are often categorized into one of two groups according to their lifecycle. Phages are classified as either lytic (virulent) or lysogenic (temperate) (Ambroa et al., 2020; Clokie et al., 2011). Strictly lytic phages are preferred for therapeutic applications, due to their ability to infect and lyse target bacteria (Figure 2). The detailed life cycle of lytic and temperate phages are depicted in Figure 2.

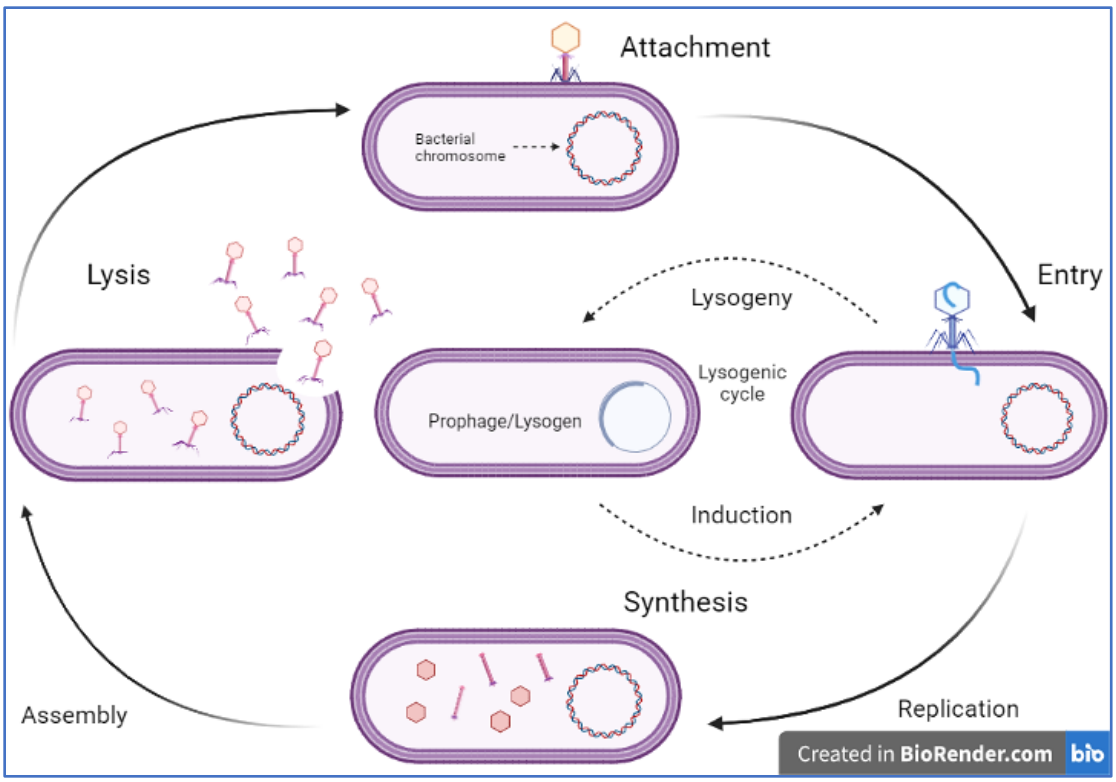

Figure 2: Phage Life cycle. Adapted from Campbell, (2003).

Opposed to the direct lysis of a bacterial host through lytic pathways, temperate phages are unique in their ability to enter a lysogenic cycle. During lysogeny, a phage will integrate its genome into the host chromosome to be replicated vertically along with the bacterium in the form of a prophage (Figure 2). Bacterial host cells that carry an integrated prophage are termed 'lysogens' due to the potential for phage induction and lysis (Casjens, 2003) (Figure 2). Lysogenic conversion genes, those that are expressed from the donating prophage, can modify the properties of the host bacterium (Brüssow et al., 2004; Casjens et al, 2003; Casjens and Hendrix, 2003). The horizontal transfer of lysogenic conversion genes is of concern and may impart determinants of resistance that enhance the virulence of recipient bacterial hosts (Boyd and Brüssow, 2002; Casjens, 2003). On some occasions, cells containing a prophage may release intact phage virions through the lytic cycle in a process referred to as induction (Casjens, 2003) (Figure 2). Induction of prophages may occur spontaneously and randomly, but is often ascribed to specific environmental cues, including

changes in nutrient availability, osmolarity, and temperature (Casjens, 2003; Lunde et al., 2005; Matos et al., 2013).

Phage Therapy

The use of phage therapy in humans has been successful (Duplessis et al., 2018; Fish et al., 2018, 2018b; Khawaldeh et al., 2011; McCallin et al., 2019; McCutcheon and Dennis, 2021). The safety of phage therapy application has been documented, with few side effects or immune responses reported during or after administration of phage (Rhoads et al., 2009; Wright et al., 2009). Phage treatments in animal models of infection have shown to be more effective, exhibit little or no toxicity, and are cheaper due to shorter treatment periods, compared to antibiotic regimens (Alemayehu et al., 2012; Agarwal et al., 2018; de Oliveira et al., 2020). Recent animal models and clinical trials have shown phage therapy to be a potential treatment for infections caused by MDR bacteria (Peters et al., 2020; Wright et al., 2009; Zhang et al., 2013). Several requirements, including FDA approval for the use of phages, are requisite to implement such a strategy in clinical trials (Parracho et al., 2012; Wienhold et al., 2019).

It is essential that all phages be fully characterized before being considered for therapeutic applications. Thorough description of a phage's biological properties is generally accomplished through complete genome sequencing, functionality testing, host range analysis, and microscopic imaging. Screening of a newly isolated bacteriophage must demonstrate that the phage possesses certain properties suitable for therapy (Abedon and Thomas-Abedon, 2010; Hyman, 2019). These include features such as the ability to lyse target bacterial pathogens through a lytic lifecycle. As previously mentioned, characterization of the bacteriophage genome is also necessary to ensure that phages are non-hazardous and unable to contradict the efficacy of therapy through horizontal gene transfer (Hyman, 2019; Lee et al., 2014; Peters et al., 2018, 2019, 2020; Petrova et al., 2014).

S. maltophilia Bacteriophages

Several lytic phages characterized against *S. maltophilia* have been isolated from environmental sources, including soil (McCutcheon et al., 2020; Peters et al., 2015; Peters et al., 2018; Peters et al., 2019, Peters et al., 2020) and sewage (Chang et al., 2005; Chen et al., 2007; Fan et al., 2012; García et al., 2008; Huang et al., 2012; Zhang et al., 2021). In addition, temperate *S. maltophilia* phages have been isolated from prophage induction (García et al., 2008; Hagemann et al., 2006; Petrova et al., 2014). Use of temperate *S. maltophilia* phages is limited based on their potential to form stable prophages, transfer resistance determinants, and enhance the virulence of bacterial hosts. Yet, characterization of temperate phages remains valuable, and researchers are investigating the prospects of genetic manipulation to enhance their utility in phage therapy (Gill and Hyman 2010; Hyman, 2019).

The first report of a phage isolated against *S. maltophilia*, φSMA5, was published in 2005 (Chang et al., 2005). Since the isolation of φSMA5, increases in the prevalence of *S. maltophilia* infections and rising drug resistance have created a demand for the identification of additional phages targeting this bacterium. To date, *S. maltophilia* has shown susceptibility to a relatively small number of known phages; at the time of writing, none of these phages have been used in therapy against infections caused by *S. maltophilia* (McCutcheon and Dennis, 2021). As the demand for alternative antimicrobial strategies remains high, documentation of *S. maltophilia* phages, and the expansion of this collection, are necessary to spearhead the clinical translation of phage therapy.

III. Materials and Methods

Materials

Unless otherwise stated, all media used for the cultivation of bacteria were either Luria-Bertani (LB) broth or LB agar (Fisher BioReagents™, Lennox) and both media were obtained from Fisher Scientific (ThermoFisher, Waltham, MA, USA). Restriction enzymes and other reagents used for DNA isolation, purification, and analysis were from Invitrogen (Invitrogen Corp., Carlsbad, CA, USA), Norgen Biotek (Norgen Biotek Corp., Thorold, Ontario, Canada) or Promega (Promega Corp., Madison, WI, USA) and obtained through Fisher Scientific. All other general reagents used in media preparation were obtained through Fisher Scientific or Sigma-Aldrich (Sigma, St. Louis, MO, USA).

Bacterial Growth Conditions

All *S. maltophilia* cultures were grown in ½ LB broth or on ½ LB agar plates unless otherwise specified. Stains of other bacterial species used in host range analysis were grown similarly in LB broth or on LB agar plates. Bacterial cultures were grown overnight for 18 h in LB medium at 37°C, with agitation of 225 rpm. Using a spectrophotometer (DU 530, Beckman, Brea, CA, USA), overnight cultures were standardized to an optical density (OD_{600}) of 1.0 by dilution with fresh LB. Aliquots of standardized cultures then were added to fresh LB and grown at 37°C with agitation of 225 rpm, until a logarithmic growth stage was reached. Overnight cultures of *S. maltophilia* were prepared in this manner unless otherwise noted and were used for the isolation of bacteriophage, phage purification, high titer enumeration, host range analysis, efficiency of plating (EOP), stability experiments, and adsorption assays.

Isolation of Bacteriophage

Samples of soil and root material were collected and used for the isolation of bacteriophages. Samples were examined for the presence of *S. maltophilia* bacteriophages using a modified phage enrichment technique (Seed and Dennis, 2005; García et al., 2008). To isolate phages from the environment, a 10 g sample of soil was suspended in 15 ml of LB broth and dispersed by shaking for 30 min at 30ºC. The soil particles were allowed to settle, removed by centrifugation at 4,000 x g for 30 min, and the supernatant filter-sterilized using a Millex-HA 0.45 µm syringe-driven filter unit (Syringe: Luer- Lok Tip, BD Falcon, NJ, USA; Filter: Whatman, GE Healthcare, Buckinghamshire, UK). Two milliliter aliquots of the filtrate were added to three ml LB medium, along with 25 µl of an *S. maltophilia* K279a overnight culture as an enrichment. This mixture was then incubated statically for 18 h at 30ºC (stability of the phage at 37ºC was not yet determined). The bacterial cells were then removed by centrifugation at 4,000 x g for 30 min and the supernatant filter-sterilized (0.45 µm). The enriched phage sample was used for corresponding plaque assays using the double-layer agar method (Peters et al., 2015; Seed and Dennis, 2005).

Plaque Assays

Plaque assays were performed by adding 200 µl of phage filtrate to 100 µl of a standardized *S. maltophilia* K279a culture grown to logarithmic phase. Mixtures were incubated for 15 min at room temperature to facilitate attachment of phage. The soft agar overlay technique was used for plating of bacterial-phage mixtures to obtain isolated plaques on lawns of target bacteria (Seed and Dennis, 2005). After 15 min of incubation, mixtures were added to four ml of sterile, molten LB soft agar (0.7% agar), swirled, overlaid on LB agar plates, and left to solidify at room temperature (Seed and Dennis, 2005). Bacteriophage plaques were identified after incubation for 24 h at 37ºC.

Plaque Purification

Isolated plaques were identified and picked for purification to obtain a uniform phage stock. A single isolated plaque was picked by touching a sterile glass Pasteur pipette to it and submerging the pipette tip into 1.5 ml of suspension media (SM) (50 mM Tris/HCl, pH 7.5, 100 mM NaCl, 10 mM $MgSO_4$) (Peters et al., 2015; Seed and Dennis, 2005). Twenty microliters of chloroform ($CHCl_3$) were added to the suspension and left for one hour at room temperature to kill any remaining bacteria (Seed and Dennis, 2005). This suspension was stored at 4°C and used in subsequent plaque assays. Three rounds of picking plaques, followed by double-layer plaque assays, were performed to produce a pure homogenous stock of Bfi2.

Generation of High Titer Phage Stock

High titer phage stocks were prepared by adding 100 µL of a standardized K279a culture grown to logarithmic phase, to 400 µL of purified phage stock, followed by incubation at room temperature for 15 min to facilitate phage attachment. Double-layer plaque assays were performed to produce plates with confluent lysis (Peters et al., 2015; Seed and Dennis, 2005). Plates with confluent lysis, where bacterial growth had been completely inhibited by Bfi2, were identified after incubation for 24 h at 37ºC.

High titer stocks of Bfi2 were generated from overlays displaying confluent lysis by adding 10 ml of SM (50 mM Tris/HCL, pH 7.5, 100 mM NaCl, 10 mM $MgSO_4$) and mixing for 2 h on a platform rocker (Stovall, Belly Dancer) at room temperature with light shaking. The lysate was recovered, centrifuged for five min at 10,000 x g, filter-sterilized (0.45 µm), and stored at 4°C for use as a working phage stock (Peters et al., 2015). The titer for the phage stock was determined from plaque assays using serial dilutions of the high titer phage stock into SM to obtain countable numbers of plaque-forming units (PFU). High titer phage stocks were stored long-term at -80°C

for future use. Titers were calculated from plaque assays performed in experimental and biological triplicate. Phage stock titer (PFU/ml) was calculated using the following equation:

PFU/ml = ((Number of plaques counted) (Dilution factor))/ (Volume plated (ml))

Host Range Analysis

Host range analysis of Bfi2 was performed using the spot test method (García et al., 2008; Peters et al., 2015, 2020). Spot tests were conducted against a panel of ten *S. maltophilia* strains of clinical and environmental origin (Table 2). Extended host range analysis was also performed against a collection of *P. aeruginosa*, *Staphylococcus aureus*, and *Escherichia coli* strains (Table 2). For spot tests, each test strain was cultured overnight, standardized, and grown to logarithmic phase as previously described. Sterile wooden cotton swabs were used to spread a uniform layer of bacterial culture onto LB agar plates. A total of four 5 µL drops of high titer phage stock (10^{11} PFU/ml) were individually placed at each corner of the agar plate. Aliquots of phage stock were allowed to absorb into the agar at room temperature and plates were then incubated for 24 h at 37°C. Plates were inspected for zones of clearing, indicating successful infection by Bfi2. Spot tests for each test strain were performed in biological and experimental triplicate.

Bacterial Strains
S. maltophilia
ATCC 13637
ATCC 17807
F6466
F7221
H59296
JB 10-15
JB 12-23
K279a
S18202
X26332
P. aeruginosa
PAO1
ATCC 22580
ATCC 27583
ATCC 27853
E. coli
JM109
ATCC 25922
S. aureus
ATCC 29213
ATCC 25923

Table 2: Bacterial Strains Used in Spot Tests for Host Range Analysis.

Efficiency of Plating (EOP) Analysis

The efficiency of plating (EOP) of the phage was performed using double-layer plaque assays according to a previously described protocol, with modifications (de Melo et al., 2019; Khan Mirzaei and Nilsson, 2015). Plaque assays were performed to quantify phage Bfi2 titers against various *S. maltophilia* strains found to be susceptible during spot tests. EOP values were calculated as the ratio of average phage titer formed on the test strain against the average titer on the host strain K279a (Khan Mirzaei and Nilsson, 2015). The EOP of Bfi2 against each test strain was reported on a relative scale, with the host strain K279a assigned an EOP value of 1.0. The isolated phage was tested in biological and experimental triplicate against each *S. maltophilia*

strain found to be susceptible during the preliminary host range spot tests. Data were analyzed using GraphPad Prism 8 (GraphPad Software Inc., San Diego, CA, USA).

Electron Microscopy

Phage ultrastructure was analyzed at the Imaging Facility of Loyola University, at the Chicago Health Sciences campus, Maywood, Illinois. High titer phage samples (10^{11} PFU/ml) were concentrated using Amicon-100 centrifuge filtration units (Bio-Rad, Techview, Singapore) and washed three times with modified SM (50 mM Tris/HCL, pH 7.5, 10 mM $MgSO_4$) (Yang et al., 2010). Samples of phage were prepared for imaging using carbon-coated 200 mesh copper grids (Ted Pella Inc., Redding, CA, USA). Copper grids were treated with 0.002% alcian blue in 0.03% acetic acid (Electron Microscopy Sciences, Hatfield, PA, USA) for five min to increase grid hydrophobicity. Grids were then washed by incubation with distilled water for five min, incubated with a high titer phage stock (10^{11} PFU/ml), and then stained with 1% (wt/vol) uranyl acetate. Phage samples were imaged using a Philips CM120 transmission electron microscope (Voltage= 80kV) equipped with an AMT Biosprint camera. Images of eleven individual virions were used for the measurements of the Bfi2 ultrastructure. Measurements for the diameter of the capsid head, along with the phage tail length and width were taken using ImageJ software (Schneider et al., 2012).

Bacteriophage DNA Analysis

Bfi2 phage DNA was isolated using the Phage Genomic DNA Isolation Kit according to the manufacturer's instructions (Norgen Biotek Company, Thorold, Canada). The concentration of the isolated DNA was determined using a Nanodrop 2000c (ThermoFisher). Purified phage DNA was subjected to restriction enzyme digestion with type II endonucleases (Table 3), based on their ability to digest double-stranded (ds) DNA. Approximately 150-200 ng of purified phage

DNA was used to prepare each digest. Digested DNA was then separated on an agarose (1.0%) (ThermoFisher) gel at a constant current of 125 mA for 1.5 h (Powerpac Basic, Bio-Rad, Techview, Singapore). Visualization of digests was performed on an Odyssey Fc Imager with an exposure time of 2 min at the 600 nm channel (LI-COR Biosciences, Lincoln, NE, USA). The gel was then analyzed using ImageJ software and the size of phage genomic DNA was estimated based on comparisons to a standard curve of the molecular weight (MW) marker (1kb).

Restriction Enzymes (REs)	
BgIII	PvuII
ClaI	SmaI
EcoRI	SalI
HindIII	XbaI
PstI	XhoI

Table 3: Type II Restriction Enzymes Used to Digest Phage Bfi2 DNA.

SDS-PAGE

Bfi2 Phage proteins were characterized by SDS-PAGE using 10% Mini-Protean GTX precast gels (Bio-Rad, Techview, Singapore). Phage samples (10^{11} PFU/ml) were purified using Amicon-100 centrifuge filtration units and washed three times with modified SM buffer (50 mM Tris/HCL, pH 7.5, 10 mM $MgSO_4$) (Yang et al., 2010). Aliquots of concentrated phage (12.5 µl), containing ~3 µg of total phage protein, were mixed 1:1 with 2x sample buffer (2X Laemmli, 5% β-mercaptoethanol, Bio-Rad, Techview, Singapore), boiled for 5 min, and loaded for a final volume of 25 µl/well. Conversely, 5 µl MW marker, containing ~3 µg of total protein, was loaded into the appropriate wells (Unstained SDS-PAGE Standards, broad range, 200 µl, Bio-Rad, Techview, Singapore). Proteins were separated at a constant voltage of 100V for 30 min, followed

by continued separation at a constant current of 85 mA for 1 h (Powerpac Basic, Bio-Rad, Techview, Singapore). Separated protein bands were visualized by staining with Coomassie Brilliant Blue G-250. The gel was then de-stained overnight (glacial acetic acid, methanol) and imaged using an Odyssey FC imager (LI-COR Biosciences, Lincoln, NE, USA) on a white-light background. The sizes of separated proteins were estimated using ImageJ software based on comparisons to a standard curve of the MW marker (6.5 - 200 kDa).

Sensitivity of Phage to pH and Temperature

The sensitivity of Bfi2 to different storage conditions was assessed according to previously described protocols (Danis-Wlodarczyk et al., 2015; Gallagher et al., 2005; Yang et al., 2010). Sensitivity to heat was determined by incubation of dilutions of high titer phage stock (10^{11} PFU/ml) at temperatures of 30°C, 50°C, and 60°C at a standard pH of 7.5. Samples were taken at 30 min intervals over the course of two hours for 30 and 50°C. Conversely, samples were taken at 5 min intervals over the course of 20 min for 60°C. After each interval, phage samples were taken and titers determined through plaque assays performed with the host strain K279a, as previously described. Phage sensitivity to pH was determined by incubation of high titer phage stock (10^{11} PFU/ml) dilutions in modified SM (50 mM Tris/HCL, pH 7.5, 10 mM $MgSO_4$) prepared at pH of 5, 7, and 9 (pH adjusted with HCl). Samples of phage incubated in each pH condition were taken at 30 min intervals over the course of 2 h at room temperature. Phage titers were determined through plaque assays with the host strain K279a, as previously described. All experiments were performed in biological and experimental triplicate. Data were analyzed using GraphPad Prism 8 (GraphPad Software Inc., San Diego, CA, USA). Two-Way ANOVAs were used to compare mean phage titer in response to temperatures of 30ºC, 50ºC, and 60°C, as well as at pH 5, 7, and 9, over time. One-way ANOVAs were used to compare the differences in mean

phage titer over the duration of the experimental conditions at 30°C, 50°C, and 60°C, respectively. Dunnett's multiple comparisons were used to compare significant differences between experimental groups to the control (Phage titer at time zero).

Adsorption Assay

The kinetics of phage adsorption to the host strain *S. maltophilia* K279a were determined following a previously outlined protocol, with modifications (Ahern et al., 2014; Chang et al., 2005; Shao and Wang, 2008). Liquid cultures of logarithmically growing *S. maltophilia* K279a cells were infected with phage at a multiplicity of infection (MOI) of ~0.05. The bacterial-phage mixtures were incubated at 30°C with shaking and samples (500 µL) were taken at five-min intervals for 15 min. At each time interval, samples were immediately diluted to halt adsorption and then centrifuged at 12,000 x g for 2 min to remove attached phage. Titers of unadsorbed phage were determined from centrifuged samples through plaque assays as previously described. Adsorption curves were generated from two independent experiments performed in triplicate and the amount of unadsorbed phage was averaged and reported as a percentage of initial phage titer.

The adsorption rate constant (k) was also determined and calculated according to established technique (Ahern et al., 2014; Shao and Wang, 2008). The rate of phage disappearance can be defined using the equation $dP/dt = -kBP$, where B is the concentration of bacteria, P is the concentration of phage at any time (t), and the adsorption rate constant (k) is expressed in ml min^{-1} (Ahern et al., 2014; Schwartz, 1976). Adsorption rate constants have traditionally been estimated by fitting a linear regression line to curves of experimentally determined phage concentrations. Therefore, the slope of the regression line is a product of the phage adsorption rate constant (k) and bacterial cell concentration (B). Assuming constant cell density, the adsorption rate constant

was estimated by dividing the product of the slope by the bacterial cell concentration (Shao and Wang, 2008).

IV. Results

Isolation of *S. maltophilia* Bacteriophage

The bacteriophage (Bfi2) was obtained from soil samples containing root material from the surrounding Chicago, Illinois area. Bfi2 was propagated using conventional enrichment techniques and isolated with standard double-layer plaque assays (Hyman and Abedon, 2009; Kropinski et al., 2009; Seed and Dennis, 2005). *S. maltophilia* strain K279a was used as the host strain for isolation and purification. Bfi2 produced clear plaques with well-defined morphology on lawns of *S. maltophilia* K279a (Figure 3). Measurements of 10 individual plaques from the initial plate of isolation with the host strain revealed an average plaque diameter of ~1.2 mm.

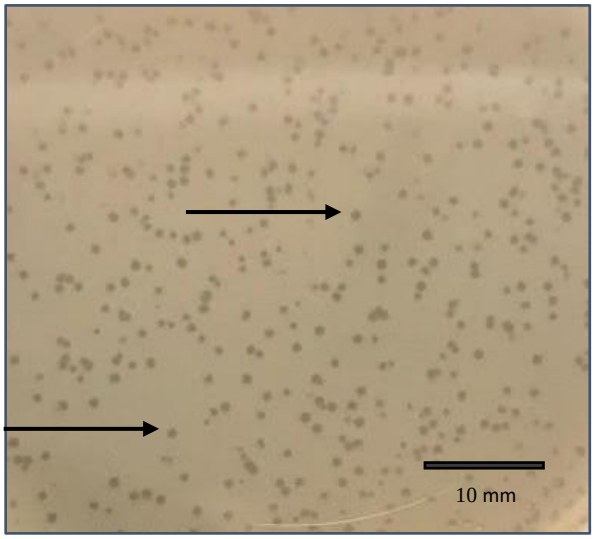

Figure 3: Plaques Formed by Bfi2 during the First Round of Isolation. Plaques formed by Bfi2 on lawns of *S. maltophilia* strain K279a after 18 h incubation at 37°C. Arrows designate typical plaques of Bfi2. Scale bar = 10 mm.

Plaque Morphology and Enumeration of Phage Titer

Double-layer plaque assays with dilutions of purified phage stock were performed to determine viral titer. The titer of the purified phage stock was calculated using the aforementioned equation (See Materials and Methods: Generation of High Titer Phage Stock) and estimated to be ~1.73 ± 0.38 x 10^{11} PFU/ml. Plaque assays with *S. maltophilia* strain K279a and preparations of purified phage resulted in different plaque morphology at 30°C and 37°C, with larger plaques formed at 30°C ($t_{(38)} = 2.45$, $P < 0.05$) (Figure 4). Measurements of 20 individual plaques were taken from two separate plates after overnight incubation at each temperature. Bfi2 was found to form plaques with an average diameter of ~1.23 mm at 37°C, compared to ~1.46 mm at 30°C.

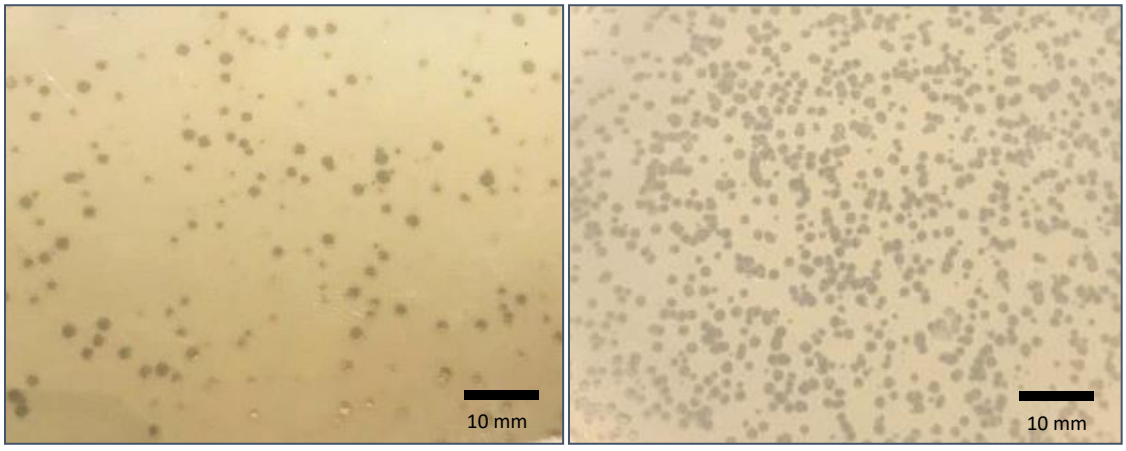

Figure 4: Plaque Morphology of Phage Bfi2. Plaque morphology on lawns of *S. maltophilia* strain K279a at 30°C (left) and 37°C (right) after 18 h incubation. Scale bar = 10 mm.

Host Range Analysis

Direct Spot Tests

The host range of Bfi2 was assessed through direct spot tests using a collection of bacterial strains including *S. maltophilia*, *P. aeruginosa, E. coli,* and *S. aureus* (Table 4). These pathogens are frequently co-isolated with *S. maltophilia* or associated with respiratory infections in humans, and were used to assess the phage's ability to infect bacteria across taxonomic orders (Brooke, 2012; Peters et al., 2015, 2017; McCutcheon et al., 2020). Phage Bfi2 demonstrated a moderate host range across the *S. maltophilia* strains tested, with the ability to infect and form zones of

clearing on six of the 11 (55%) strains during spot tests (Table 4). Dependent on the strain, Bfi2 was initially shown to form clear (4/11) and turbid plaques (2/11) on strains of *S. maltophilia*. Later assays determined that Bfi2 could reliably form plaques on only two of the six susceptible *S. maltophilia* strains, K279a and F7221. It is possible that strain-specific differences in the structure and expression of cell surface receptors account for the turbid plaques formed by Bfi2. This reduction in plaquing ability has been observed for other phages and may also be explained by the repeated propagation of a phage on its host strain (Peters et al., 2020). The propagation of Bfi2 on a single host strain may have selected for phage variants that are optimized to K279a over time. Bfi2 showed the ability to infect both clinical and environmental isolates of *S. maltophilia*. However, Bfi2 did not show cross-taxonomic order infectivity and was unable to form zones of clearing in the lawns of the other Gram-positive and Gram-negative bacterial species tested (Table 4).

Host Range Analysis		
Strain	Phage Infection	Plaque Morphology
S. maltophilia		
ATCC 13637	+	***clear***
ATCC 17807	+	***turbid***
F64644	-	*NA*
F7221	+	***clear***
H46033	-	*NA*
H59296	+	***clear***
JB 10-15	-	*NA*
JB 12-23	-	*NA*
K279a	+	***clear***
S18202	+	***turbid***
X26332	-	*NA*
P. aeruginosa		
ATCC 22580	-	*NA*
ATCC 27853	-	
PAO1	-	
E. coli		
ATCC 25922	-	*NA*
JM109	-	
S. aureus		
ATCC 25923	-	*NA*
ATCC 29213	-	
Infection= (+) ; No Infection= (-)		

Table 4: Host Range Analysis of Phage Bfi2 against a Collection of *S. maltophilia* Strains and Co-isolated Pathogens. Results are representative of host range spot tests performed in experimental and biological triplicate; plates were incubated for 18 h at 37°C and observed for zones of clearing. NA, not applicable.

Efficiency of Plating (EOP)

The efficiency of plating (EOP) was used to quantify the ability of the isolated phage to infect different *S. maltophilia* isolates, which provided a more accurate representation of relative lytic activity. EOP for Bfi2 was tested via plaque assays with *S. maltophilia* strains that were found to be susceptible during initial spot tests. Yet, plaque formation was observed only on lawns of two clinical strains of *S. maltophilia*, K279a and F7221, during preliminary EOP assays. EOP values were obtained by comparison of phage titer observed on the test strain to the titer on the host strain K279a (EOP value of 1.0). These assays shown Bfi2 to be nearly half as effective

against F722l (EOP value of 0.48) compared to the host strain K279a used for initial isolation (Figure 5).

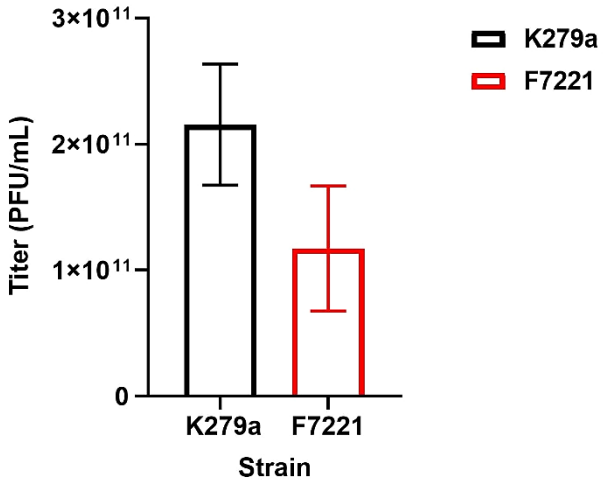

Figure 5: Phage Bfi2 Efficiency of Plating (EOP) Analysis. Phage titers were obtained from EOP assays between *S. maltophilia* strain F7221 and host strain K279a. EOP values were calculated as the ratio of Bfi2 titer against the test strain to the titer observed on the host strain (value of 1.0), reported on a relative scale.

Transmission Electron Microscopy (TEM)

Micrographs of Bfi2 revealed an icosahedral capsid with well-defined edges that measured 75.3 ± 3.3 nm in length and 69.5 ± 3.9 nm in width. The phage tail was flexible, non-contractile, and measured 154.2 ± 4.6 nm in length and 9.3 ± 0.5 nm in width. Morphological analysis of individual phages suggests that Bfi2 ultrastructure is consistent with members of the family *Siphoviridae*. Based on the International Committee on Taxonomy of Viruses (ICTV) classification scheme, Bfi2 may be further be identified as a B1 morphotype within the family *Siphoviridae* due to its relative dimensions, isometric capsid, flexible non-contractile tail, and absence of tail fibers (Ackermann, 1998; Ackermann and Eisenstark, 1974; Chibani et al., 2019).

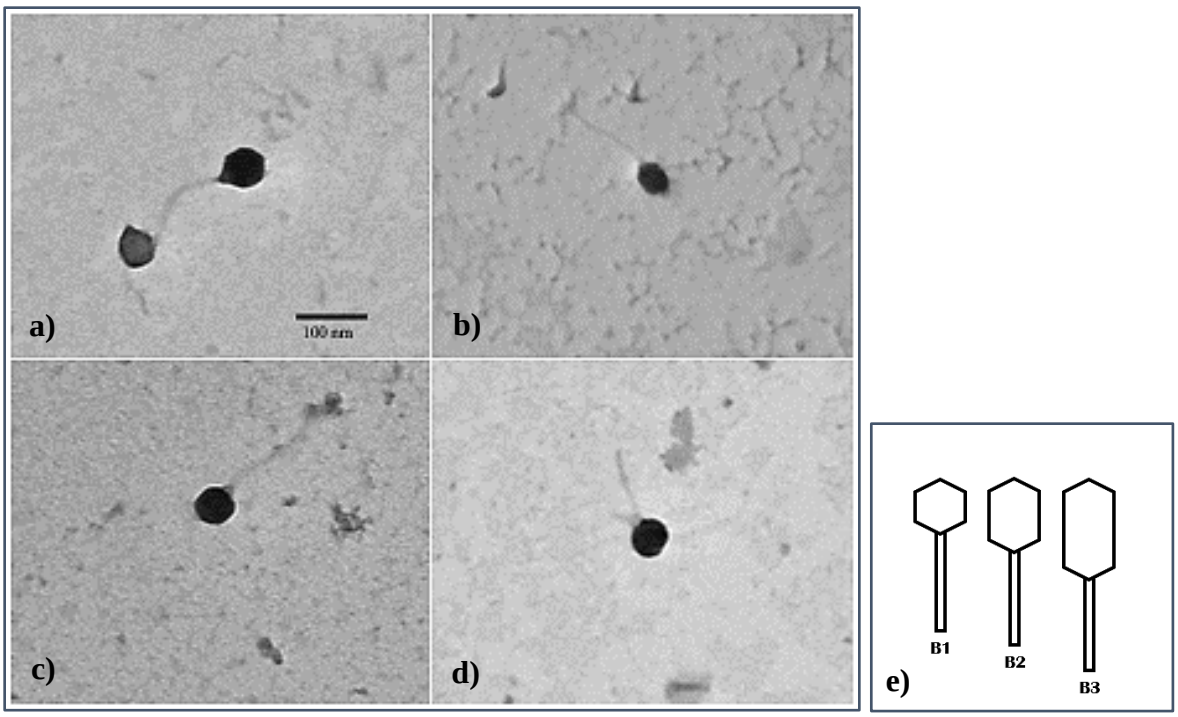

Figure 6: Transmission Electron Micrograph of Phage Bfi2 Morphology. Prepared phage lysate was added to carbon coated copper grids and negatively stained with 1% uranyl acetate. TEM images were obtained at magnifications of **a)** 35,000x, **b)** 17,000x, **c)** 22,000x, and **d)** 28,000x. Phage ultrastructure measurements of capsid length, capsid width, tail length, and tail width were taken as the average from individual virions (n = 11). Scale bar = 100 nm. **e)** Morphotypes of phages within the family *Siphoviridae;* Adapted from Ackermann, 1998.

Phage Genome Analysis

Phage nucleic acid was isolated and purified, subjected to restriction enzyme digestion, and products were visualized by agarose gel electrophoresis. The Bfi2 genome was confirmed to be composed of DNA based on the ability of type II endonucleases to digest double-stranded (ds) DNA. Only two (EcoRI and PvuII) of the ten tested restriction enzymes [BgIII, ClaI, EcoRI, HindIII, PstI, PvuII, SmaI, SalI, XbaI, XhoI] were able to digest the DNA of Bfi2 (Table 5, Figure 7). However, digestion with EcoRI and PvuII produced clear and well-separated bands (Figure 7). The size of the Bfi2 genome from each restriction reaction was calculated by summation of the DNA fragments. The size of the Bfi2 phage genome was determined using the average from the two successful RE digests and was estimated to be approximately 66.5 kbp (Table 5). However,

due to the preliminary nature of this data, complete genome sequencing is necessary to confirm this estimate.

Band	EcoRI (bp)	PvuII (bp)
1	11814	12171
2	8769	10486
3	7784	9308
4	6706	6909
5	5128	5952
6	4552	4552
7	3586	4289
8	3183	3922
9	2363	3586
10	2097	2826
11	1862	1862
12	1511	1652
13	1190	1155
14	910	761
15	717	472
16	532	
17	445	
Total	63158	69910
Average		66534

Table 5: Phage Bfi2 DNA Fragment Sizes from Restriction Enzyme Digests. Isolated Phage DNA was subjected to RE digestion with EcoRI and PvuII at 37°C for 1 h. Digested DNA was separated on a 1.0% agarose gel at a constant current of 125 mA for 1.5 h. Fragment band sizes were estimated from comparisons to a standard curve of the MW marker (1kb).

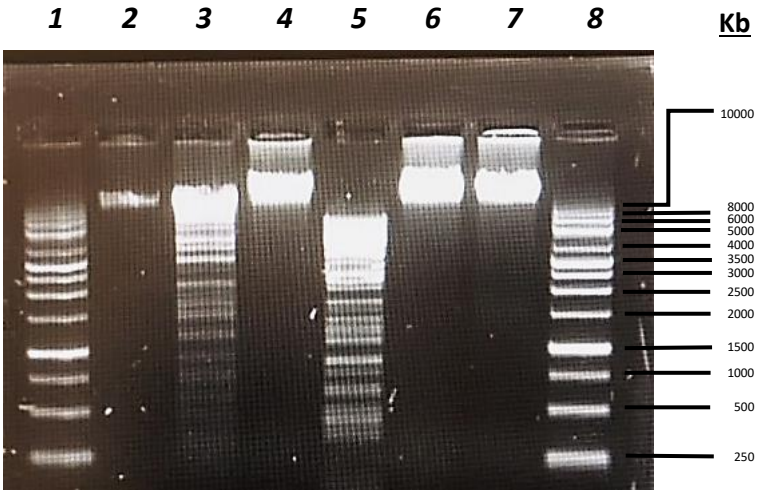

Figure 7: Visualization of Isolated Phage DNA Restriction Enzyme Digests. Lanes are as follows: (1) 1 kb ladder, (2) Uncut phage DNA, (3) EcoRI, (4) KpnI, (5) PvuII, (6) SmaI, (7) SphI, (8) 1 kb ladder.

SDS-PAGE

To further characterize Bfi2 phage, structural proteins were isolated and analyzed by SDS-PAGE (10% polyacrylamide gel) and stained with Coomassie blue. At least four distinct protein bands were visualized (P1-P4), with an estimated 12-kDa protein being the most abundant component of the Bfi2 phage particle (Figure 8; P3). Two additional protein bands of low intensity, P2 and P4, were estimated to be approximately 23-kDa and 8-kDa, respectively. A faint protein band of larger size was also visible and estimated to be approximately 86-kDa (Figure 8; P1).

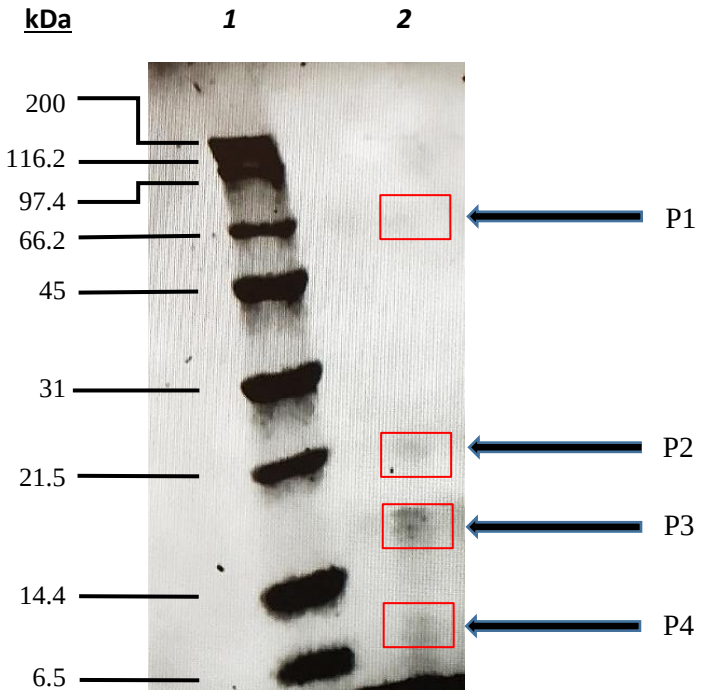

Figure 8: Analysis of Phage Bfi2 Structural Proteins by SDS-PAGE. Approximately 3 µg of total phage protein was loaded into the appropriate wells. Conversely, 5 µl MW marker was loaded into the appropriate wells (Unstained SDS-PAGE Standards, broad range, 200 µl, Bio-Rad). Lanes are as follows: (1) MW marker, (2) concentrated phage proteins.

Structural Stability of Phage in Response to Environmental Conditions

Phage Stability in Response to Temperature

Thermal stability assays were performed to analyze the structural stability of Bfi2 in response to heat at a standard pH of 7.5. Phage thermostability was assessed by double-layer plaque assays over the course of a two-hour incubation period at temperatures of 30°C, 50°C, and 60°C (Figure 9). Preliminary studies revealed phage activity to decrease drastically after 30 minutes of incubation at 60°C (Figure 9a). Therefore, stability assays at 60°C were amended to cover a 20-minute incubation period (Figure 9b). A one-way ANOVA was used to compare the effect of time on phage titer after incubation at 60°C. Time was found to significantly affect phage titer after incubation at 60°C over the duration of the experiment ($F_{(1.37, 10.99)} = 83.11$, $P < 0.0001$) (Figure 9b). Posthoc Dunnett's multiple comparisons on the effect of time at 60°C revealed a significant difference between phage titer at 5 minutes ($P < 0.0001$), 10 minutes ($P < 0.0001$), 15

minutes ($P < 0.0001$), and 20 minutes ($P < 0.0001$), compared to the control (Titer at time zero) (Figure 9b). Moreover, phage titer decreased by > 1.5 log units (~17%) after 20 minutes of incubation at 60°C, compared to the control (Titer at time zero) (Figure 9b).

A two-way ANOVA was used to compare mean phage titer after incubation at 30ºC, 50ºC, and 60ºC. A significant effect of the interaction between temperature and time ($F_{(8, 96)} = 76.97$, $P < 0.0001$) on phage titer was observed after incubation at 30ºC, 50ºC, and 60ºC. Due to the significant interaction between these variables, it is difficult to interpret the individual effect of temperature treatment on phage titer.

One-way ANOVAs were then used to independently compare the effects of time on phage titer after incubation at each respective temperature. Analysis determined that time did not significantly affect phage titer at 30°C during the incubation period ($F_{(1.66, 13.3)} = 2.419$, $P > 0.05$). However, a one-way ANOVA determined that time significantly affected phage titer after incubation at 50°C over the duration of the experiment ($F_{(2.26, 18.1)} = 79.48$, $P < 0.0001$). Posthoc Dunnett's multiple comparisons of the time effect at 50°C showed no significant difference in phage titer after 30 minutes of incubation compared to the control ($P > 0.05$) (Titer at time zero) (Figure 9a). Yet, time appears to drive the effect of temperature, as Dunnet's multiple comparisons revealed a significant effect of time on phage titer after 60 minutes ($P < 0.0001$), 90 minutes ($P < 0.0001$), and 120 minutes ($P < 0.0001$) of incubation at 50°C, compared to the control (Titer at time zero) (Figure 9a). Moreover, after two hours of incubation at 50ºC, phage titer decreased < 1.0 log units (~8%) compared to the control (Titer at time zero).

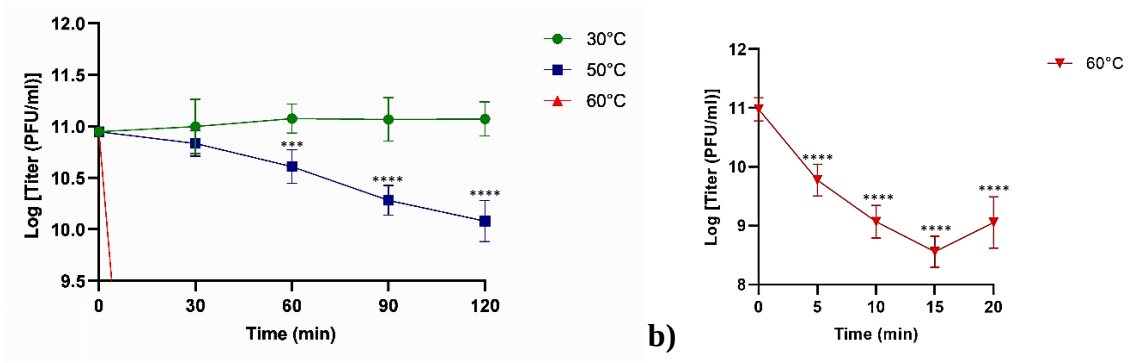

Figure 9: Stability of Phage Bfi2 in Response to Temperature. The data points are representative of phage mean titer against *S. maltophilia* K279a after incubation at each temperature **a)** 30°C, 50°C, and 60°C for the appropriate time interval (0-120 min) **b)** 60°C for the appropriate time interval (0 - 20 min). Error bars represent standard deviation. *P < 0.05, ***P < 0.0005, ****P < 0.0001 indicates a significant difference between this group and the control (Titer at time zero).

Phage Stability in Response to pH

Stability assays were performed to analyze the structural stability of the Bfi2 in response to pH at room temperature for up to two hours. The stability of Bfi2 at pH 5, 7, and 9 in modified-SM buffer was determined by analyzing phage titer in 30-minute intervals by double-layer plaque assays (Figure 10). A two-way ANOVA was used to compare mean phage titer after incubation at pH 5, 7, and 9. No significant effect of pH environment on phage titer was found after incubation at pH 5, 7, and 9 for up to two hours ($F_{(2, 24)} = 1.720$, $P > 0.05$) (Figure 10). While not statistically significant, Bfi2 titer decreased < 1.0 log unit (~10%) during the incubation period in all pH conditions.

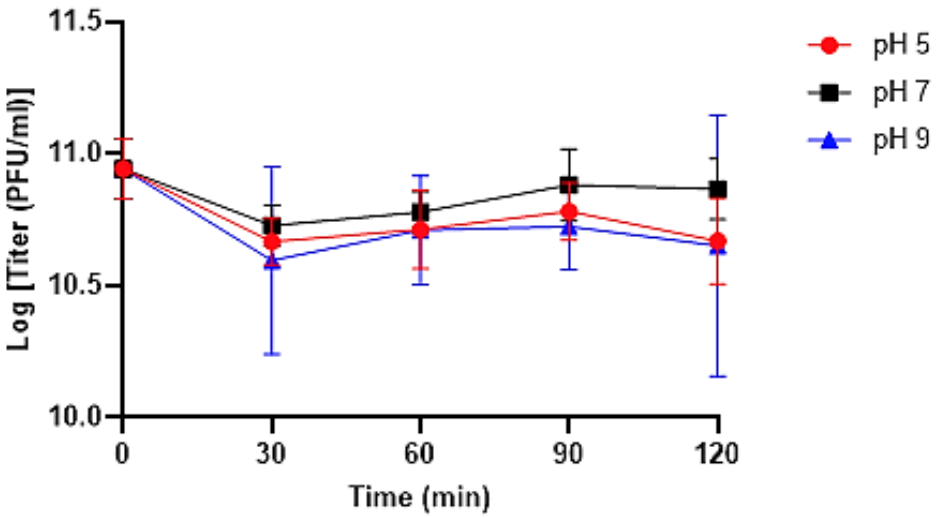

Figure 10: Stability of Phage Bfi2 in Response to pH. Data points are representative of mean phage titer against *S. maltophilia* K279a after incubation in pH buffered modified-SM for the appropriate time interval (0 - 120 min). Error bars represent standard deviation.

Phage Adsorption Assay

Adsorption assays were performed to determine the efficiency of Bfi2 to attach to host cells of *S. maltophilia* K279a, and the rate constant (*k*) of phage adsorption. Early log-phase S. *maltophilia* K279a cultures were infected with phage at a MOI of 0.05, and phage titers were quantified in five-minute intervals over the course of a 15 minute incubation period. The duration of this assay was chosen to simulate the standard incubation period promoting phage attachment to host cells prior to plating via the double-layer agar technique (See Materials and Methods: Isolation of Bacteriophage). After five minutes, the percent of unadsorbed phage was measured to be ~6.4 ± 1.2% (Figure 11). The percentage of unbound phage remained consistent from 5-10 minutes, with ~6.8 ± 1.8% of phage unadsorbed after 10 minutes of incubation. Yet, the percentage of unadsorbed phage decreased by about half from 10 to 15 minutes, where ~3.3 ± 0.5% of phage remained unbound after 15 minutes of incubation. The percentage of unadsorbed phage can be used to estimate the percentage of adsorbed phage at each time point. After 15 minutes of incubation, ~97% of phages were bound to host cells.

In addition, the phage adsorption rate constant (*k*), which defines phage affinity for a bacterial host, can be described using the equation $dP/dt = -kBP$ (See Materials and Methods: Adsorption Assays) (Ahern et al., 2014; Shao and Wang, 2008). Following this method, the adsorption rate constant (*k*) of the isolated phage was estimated to be ~ $(2.15 \pm 0.06) \times 10^{-9}$ ml min^{-1}.

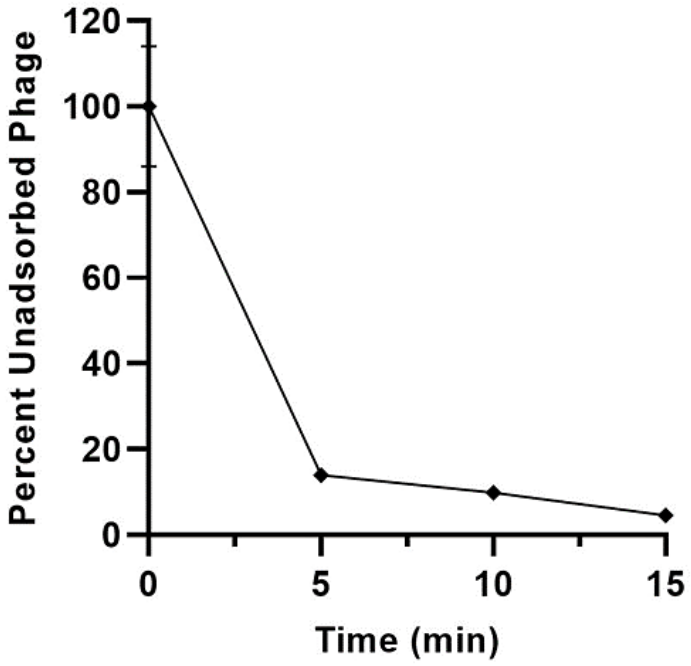

Figure 11: Adsorption Curve of Phage Bfi2 Attachment to Host Cells. The amount of unadsorbed phage was expressed as a percentage of the initial phage titer (~7.0×10^6 PFU/ml). Data points are representative of means from two independent experiments performed in triplicate. Error bars represent standard deviation.

V. Discussion

Isolation of Phage

It is a necessity that phages used for medical applications must be carefully selected and fully characterized prior to consideration. Only exclusively lytic phages should be applied and phages showing poor adsorption, replication, or distribution should be excluded from use in phage therapy (Abedon and Thomas-Abedon, 2010). This discussion will focus on the comparison between the biological characteristics of Bfi2 with those of other *S. maltophilia* phages described within the literature. An emphasis will be placed on comparisons to *S. maltophilia* phages of the family *Siphoviridae* due to the taxonomic classification of Bfi2. *S. maltophilia* phages belonging to other families with the order *Caudovirales* will be discussed when applicable. However, when little to no data are available for phages against *S. maltophilia*, phages against related, or often co-isolated, bacterial pathogens will be reviewed.

During initial isolation from the environment, Bfi2 was found to form clear and regular plaques ~1.2 mm in diameter on a lawn (confluent growth) of *S. maltophilia* K279a after incubation at 30°C. Other *S. maltophilia* phages have been observed to form plaques of smaller size (Chang et al., 2005; Peters et al., 2015; McCutcheon et al., 2020). *S. maltophilia* phages of the family *Siphoviridae* including DLP1 and AXL3, formed plaques approximately 0.7 mm and 0.78 mm in diameter, respectively (Peters et al., 2015; McCutcheon et al., 2020). Another temperate phage against *S. maltophilia*, DLP5, formed plaques approximately 0.5 mm in diameter (Peters et al., 2018). Based on these comparisons, the plaque range of Bfi2 is larger than expected for phages of the family *Siphoviridae*.

It was also interesting to observe that Bfi2 formed larger plaques at 30°C than at 37°C, with diameters of ~1.46 mm and 1.23 mm, respectively (Figure 4). Yet, the average plaque

diameter of Bfi2 at 37°C is more comparable to that of the other *S. maltophilia* siphophages described. Altered plaque morphology with regard to temperature has not been emphasized within the literature for *S. maltophilia* phages. Although more investigation is required, variations in Bfi2 plaque morphology may be explained by differences in bacterial growth rate and/or differential expression of cell surface receptors with respect to temperature (Clementz et al., 1996; Kawahara et al., 2002; Matsuura, 2013).

Moreover, plaque morphology appears to vary between lytic and temperate phages against *S. maltophilia* (Lee et al., 2014; Peters et al., 2018; Wu et al., 2021). Temperate *S. maltophilia Siphoviridae* phages have been reported to form diffuse or turbid plaques with irregular borders (Peters et al., 2018; Wu et al., 2021). It may be assumed that Bfi2 is not temperate, due to its ability to form clear and regular plaques on two separate strains of *S. maltophilia.* However, as recommended for all published *S. maltophilia* phages, further investigation into the phage lifestyle, as well as complete genomic sequencing, is required to confirm lytic nature. (McCutcheon and Dennis, 2021). Phage lifestyle can be confirmed by screening phage-resistant bacterial isolates for the presence of phage genomic DNA, which would indicate the formation of a lysogen or prophage (Peters et al., 2020). Investigation into the lifestyle of Bfi2, along with genomic sequencing, would be necessary to confirm the preliminary classification of this phage as lytic.

Aside from the determination of phage lifestyle, the additional characterization of phages allows for their classification within taxonomic orders and families based on shared similarities. Taxonomic classification and naming of virus taxa has been maintained by the International Committee on Taxonomy of Viruses (ICTV) (Adams et al., 2017; Chibani et al., 2019) and the Bacterial and Archaeal Subcommittee (BAVS) within the ICTV (Chibani et al., 2019). Classification of phages is contingent on the evaluation of a variety of properties including host

range, pathogenicity, composition of the viral genome (ss/dsDNA, RNA, and size), morphology, presence of an envelope, and sequence similarities (Chibani et al., 2019).

Host Range Analysis

The identification of phages with a broad host range is advantageous to limit the need for pathogen detection and screening that would be required to match the pathogen to a phage with specific activity (Hyman and Abedon, 2009, 2010; Weinhold et al., 2019). Use of the term "broad" to describe host range could refer to a phage's ability to infect multiple species of bacteria, or the ability to infect several strains within a species (Hyman, 2019; Ross et al,. 2016). For phage therapy, the use of broad host range phages that can infect many strains of a given species is preferable to keep normal microflora intact (Hyman, 2019).

At the time of writing, Bfi2 is the first phage to be isolated using *S. maltophilia* strain K279a as the host. Bfi2 showed the ability to infect six of 11 (55%) of the *S. maltophilia* strains tested during host range spot tests. Bfi2 possesses a moderate host range compared to the other *S. maltophilia* phages described in the literature. While the number of *S. maltophilia* strains used in this study is limited, several other virulent phages against this bacterium have shown a similar host range (Peters et al., 2017, 2018). DLP4, a temperate phage and member of the family *Siphoviridae*, showed the ability to infect 14/27 (52%) of the clinical *S. maltophilia* strains tested (Peters et al., 2018). In addition, a phage of the family *Myoviridae,* DLP6, was also found to have a moderate host range and could infect 13/27 (48%) of the clinical *S. maltophilia* strains tested (Peters et al., 2017).

A few *S. maltophilia* phages have been reported to possess a comparatively broad host range. A temperate *S. maltophilia* phage of the family *Siphoviridae*, DLP3, was observed to have a broad host range with the ability to infect 22/29 (76%) of *S. maltophilia* strains (Peters et al.,

2020). This is an interesting finding given the temperate nature of DLP3. The host range of DLP3 is one of the broadest described for any known *S. maltophilia* phage, certainly amongst those classified as a members of the family *Siphoviridae* (Chang et al., 2005; McCutcheon et al., 2020; Peters et al., 2020). For phage φSMA5, a member of the family *Myoviridae*, spot tests shown the phage to form clear and turbid zones of clearing on 61/87 (70%) and 21/87 (24%) of *S maltophilia* strains tested, respectively. To date, this is the broadest host range observed for any *S. maltophilia* phage, where only five strains were not susceptible to φSMA5 infection (Chang et al., 2005). Another recently isolated phage of the family *Myoviridae*, Ps15, displayed a broad host range and was able to infect 22/24 (90%) of *S. maltophilia* isolates associated with ocular infections (Damnjanović et al., 2022).

Phages DLP1 and DLP2, isolated against *S. maltophilia*, were found to have a relatively narrow host range (Peters et al., 2015). DLP1 and DLP2 were able to infect approximately eight (30%) and nine (33%) of the 27 *S. maltophilia* strains tested, respectively. However, DLP1 and DLP2 are the only *S. maltophilia* phages reported to be capable of infecting bacteria across taxonomic orders, where each phage could lyse two separate strains of *P. aeruginosa* (Peters et al., 2015). The ability to infect multiple species of bacteria is a rare characteristic amongst phages but this phenomenon may have important implications for therapy. Although Bfi2 was unable to infect the other species of bacteria tested, *P. aeruginosa* is often a co-colonizing pathogen associated with *S. maltophilia* infections (Moore et al., 2003; Rajan and Saiman, 2002). A phage that targets both of these species is highly desirable for the reduction of bacterial load in polymicrobial infections. However, it is important to recognize that phages with too broad a host range, that extends to include non-pathogenic bacteria, could be detrimental to therapeutic outcomes.

Efficiency of Plating (EOP) Analysis

It is worth mentioning that reviews have detailed the discrepancy between host range spot tests and efficiency of plating (EOP) assays for the determination of phage host range (Khan Mirzaei and Nilsson, 2015). Spot tests involve the administration of phage aliquots directly onto the surface of bacterial lawns. Conversely, EOP analyses typically utilize plaque assays to quantify a phage's ability to form plaques on susceptible strains of the target bacterium. Direct spot tests are prone to overestimation of phage host range and may not accurately predict the ability of a phage to form plaques on lawns of susceptible bacteria (Khan Mirzaei and Nilsson, 2015). Simply put, spot tests provide a qualitative measure of a phage's lytic activity. In contrast, the number of plaques obtained from EOP assays give a quantitative measure of a phage's relative lytic activity against bacterial test strains. Therefore, our research sought to implement both direct spot tests and EOP assays for the characterization of Bfi2 host range.

The overestimation of host range from spot tests was evident for Bfi2, where positive spot tests on lawns of *S. maltophilia* did not fully predict plaque formation during EOP assays. EOP analysis showed that Bfi2 could only form plaques on 2/6 (33%) (F7221 and K279a) of the *S. maltophilia* strains that were initially found to be susceptible from spot tests. It is interesting to note that plaque formation occurred only on lawns of clinical *S. maltophilia* strains during EOP assays. Moreover, EOP analysis showed the phage to be approximately half as effective against the test strain F722l compared to the host strain K279a used for propagation (Figure 5).

Similar discrepancies between spot tests and efficiency of plating have been observed for some *S. maltophilia* phages. The recently characterized phage BUCT598 was found to infect 9/11 (82%) *S. maltophilia* strains during direct spot tests (Han et al., 2022). Yet, EOP analysis of BUCT598 revealed that the phage could form plaques on only 33% of the nine *S. maltophilia*

strains that were previously shown to be susceptible during host range spot tests (Han et al., 2022). Similarly, phage DLP3 was reported to form zones of clearing on 22/29 (76%) of *S. maltophilia* strains tested when low dilutions of phage were applied. However, EOP analysis showed that DLP3 had a high efficiency (clearing at high dilutions of phage) against only 17.2% of the 29 *S. maltophilia* strains tested (Peters et al., 2020). Based on the data obtained for Bfi2 and other *S. maltophilia* phages, it is clear that a combination of spot tests and EOP assays should be performed to accurately assess phage host range.

Genomic Analysis

Genomic analysis confirmed the isolated phage to be composed of ds (double-stranded) DNA. To the best of our knowledge, all phages isolated and characterized against *S. maltophilia* have similarly been shown to possess DNA genomes (McCutcheon and Dennis, 2021). However, it is important to note that not all *S. maltophilia* phages have dsDNA genomes. Genomes composed of single-stranded (ss) DNA have been reported for some tailed *S. maltophilia* phages and for all filamentous phages, belonging to the family *Inoviridae* (Hagemann et al., 2006; Liu et al., 2012; Petrova et al., 2014; Wu et al., 2021) (Table 6). DNA agarose gel electrophoresis and restriction fragment length polymorphism (RFLP) analysis estimated the Bfi2 phage genome to be ~66.5 kb in size. The size of the phage genome is consistent with those of several *S. maltophilia* phages belonging to the family *Siphoviridae* (Table 6). However, complete genomic sequencing is necessary to confirm this estimate.

Two (EcoRI and PvuII) of ten restriction enzymes (REs) were shown to digest DNA isolated from Bfi2 (Figure 7). The panel of REs used in this study was limited and the genomes of other *S. maltophilia* phages have been subjected to larger collection of endonucleases (Table 5) (Chang et al., 2005; Chen et al., 2007; Peters et al., 2018, 2020). Genomic analyses of several *S.*

maltophilia phages have shown phage DNA to be completely refractory to RE digestion (Chang et al., 2005; Chen et al., 2007; García et al., 2008; Peters et al., 2020), or partially refractory (Peters et al., 2018) to RE digestion. Moreover, the genomes of a few *S. maltophilia* phages have been sequenced and analyses have confirmed the presence of modified nucleotide bases or uncommon base analogs (Chang et al., 2005; Chen et al., 2007; Peters et al., 2018, 2020). It has been suggested that modification of nucleotide bases in phage DNA may provide protection against degradation by host REs during replication (Casjens, 2003). Modified bases may also protect temperate phages during integration of the phage genome into the bacterial host chromosome (Casjens, 2003; Peters et al., 2020). A list of genomic features for published *S. maltophilia* phages is presented in Table 6.

Genomic Characteristics of Published *S. maltophilia* Phages						
Phage	*S. maltophilia* Host Strain	Genome Type	Genome Size (bp)	Origin	Country of Isolation	Reference
AXL3	D1585	dsDNA	47,545	Soil (garden)	Canada	(McCutcheon et al., 2020)
BUCT548	No. 824	dsDNA	62,354	Hospital Sewage	China	(Zhang et al., 2021)
BUCT555	No. 1207	dsDNA (linear)	39,440	Hospital Sewage	China	(Han et al., 2021)
BUCT598	No. 824	dsDNA (linear)	43, 581	Hospital Sewage	China	(Han et al., 2022)
DLP1	D1585	dsDNA	42,887	Soil (river sediment)	Canada	(Peters et al., 2015)
DLP2	D1585	dsDNA	42,593	Soil (blue flax)	Canada	(Peters et al., 2015)
DLP3	D1571[c]	dsDNA	96,852	Soil (prisine)	Canada	(Peters, et al., 2020)
DLP4	D1585	dsDNA	63,945	Soil (asparagus)	Canada	(Peters et al., 2019)
DLP5	D1614	dsDNA	96,542	Soil (garden)	Canada	(Peters et al., 2018)
DLP6	D1571[c]	dsDNA (linear)	168,489	Soil (planter)	Canada	(Peters et al., 2017)
IME13	Clinical	dsDNA (circular)	162,327	Hospital Sewage	China (Beijing)	(Fan et al., 2012)
IME15	Clinical	dsDNA (linear)	38,513	Hospital Sewage	China (Beijing)	(Huang et al., 2012)
IME-SM1	na	dsDNA (linear)	159,514	Hospital Sewage	China	(Liu et al., 2015)
Marzo	ATCC 17807[e]	dsDNA (linear)	159384	Sludge (wastewater plant, TX)	TX, USA	(Patel et al., 2022)
Mendera	ATCC 17807[e]	dsDNA (linear)	159,961	Wastewater (Navasota, TX)	TX, USA	(Garza et al., 2020)
Moby	ATCC 17807[e]	dsDNA	159,365	Wastewater (Bryan, TX)	TX, USA	(Vicary et al., 2020)
phiSHP1	P2[e]	ssDNA (circular)	6,867	*S. maltophilia* strain P2[e]	China	(Liu et al., 2012)
phiSHP3	C31	ssDNA (linear)	37,611	*S. maltophilia* strain C31	China	(Wu et al., 2021)
phiSMA5	T39[c]	dsDNA	250,000	Hospital Sewage	China	(Chang et al., 2005)
phiSMA6	TC79[c]	ssDNA	7,648	*S. maltophilia* strain Khak84[e]	Russia	(Petrova et al., 2014)
phiSMA7	TC79[c]	ssDNA	7,069	*S. maltophilia* strain Khak84[e]	Russia	(Petrova et al., 2014)
phiSMA9	C5	ssDNA (circular)	6,907	*S. malt* strain C5	Germany	(Hagemann et al., 2006)
Pokken	ATCC 17807[e]	dsDNA (linear)	76,259	Freshwater (Franklin, TX)	TX, USA	(Hayden et al., 2019)
Ponderosa	ATCC 17807[e]	dsDNA (linear)	42,612	River water sample (Zimbabwe)	TX, USA	(Marquez et al., 2019)
Ps15	AP143S	dsDNA	161,350	Wastewater (Cleveland, OH)	Australia	(Damnjanović et al., 2022)
S1	CECT 4793[e]	dsDNA	40,287	*S. maltophilia* strain A1[c]	Spain	(Garcia et al., 2008)
S2	E999[c]	na	na	*S. maltophilia* strain E539[c]	Spain	(Garcia et al., 2008)
S3	E539[c]	dsDNA **(refractory)**	33,000	Sewage	Spain	(Garcia et al., 2008)
S4	F227	dsDNA **(refractory)**	200,000	Sewage	Spain	(Garcia et al., 2008)
Salva	clinical	dsDNA (linear)	60,789	Wastewater (Cincinnati, OH)	TX, USA	(Jefferson et al., 2021)
Sm1	na	dsDNA	50,000	Hospital Sewage	China	(Zhang and Li, 2013)
smp131	T16	dsDNA	33,525	*S. maltophilia* strain T16	Taiwan	(Lee et al., 2014)
smp14	T14	dsDNA **(refractory)**	160,000	Hospital Sewage	Taiwan	(Chen et al., 2007)

Table 6: Genomic Characteristics of *S maltophilia* Phages; Strains: **[c]**, Clinical; **[e]**, Environmental.

Transmission Electron Microscopy

Transmission electron microscopy (TEM) imaging allowed for morphological analysis and measurement of the Bfi2 ultrastructure. Most importantly, Bfi2 was found to possess an icosahedral capsid with dimensions of 75.3 ± 3.3 nm in length and 69.5 ± 3.9 nm in width (Figure 6). A flexible, non-contractile tail was determined to be 154.2 ± 4.6 nm in length and 9.3 ± 0.5 nm

in width (Figure 6). Based on the relative dimensions, presence of a non-contractile tail, and absence of tail fibers, the phage could be classified as a member of the order *Caudovirales* within the family *Siphoviridae* (Figure 6). As have been reported for other *S. maltophilia* phages, the isometric capsid of Bfi2 suggests that this phage could be classified as a B1 morphotype (where the length and width of the icosahedral capsid are of similar size) within this taxonomic family (Ackermann, 1998; Ackermann and Eisenstark, 1974; Demuth et al., 1993; McCutcheon et al., 2020; Peters et al., 2018).

TEM in combination with complete genome sequencing have allowed several *S. maltophilia* phages to be classified as members of the family *Myoviridae* (Chang et al, 2005; Chen et al., 2007; Damnjanović et al., 2022; Fan et al., 2012; Huang et al., 2012; García et al., 2008; Garza et al., 2020; Lee et al., 2014; Peters et al., 2016; Vicary et al., 2020), *Siphoviridae* (Jefferson et al., 2021; McCutcheon et al., 2020; Peters et al., 2015, 2018, 2019, 2020), *Podoviridae* (Han et al., 2021, 2022; Hayden et al., 2019; Marquez et al., 2019), and *Inoviridae* (Hagemann et al., 2006; Liu et al., 2021; Petrova et al., 2014). A list of phage ultrastructure measurements and taxonomic classifications for lytic *S. maltophilia* phages is presented in Table 7. A similar list of measurements and classifications for temperate *S. maltophilia* phages is presented in Table 8. It is clear that Bfi2 is likely a member of the family *Siphoviridae* due to its similarity with other *S. maltophilia* phages belonging to this taxonomic classification.

Morphology of Lytic *S. maltophilia* Phages					
Phage	*S. maltophilia* Host Strain	Family	Ultrastructure		Source
			Capsid	*Tail*	
AXL3	D1585	*Siphoviridae*	64.3 ± 3.2 nm x 63.3 ± 4.3 nm	145.3 ± 5.4 nm	(McCutcheon et al., 2020)
BUCT548	No. 824	*Siphoviridae*	50 nm	138 nm	(Zhang et al., 2021)
BUCT555	No. 1207	*Podoviridae*	45 nm	8 nm	(Han et al., 2021)
BUCT598	No. 824	*Podoviridae*	51.77 ± 2.70 nm	9.95 ± 0.95 nm	(Han et al., 2022)
DLP1	D1585	*Siphoviridae*	70 nm	175 nm	(Peters et al., 2015)
DLP2	D1585	*Siphoviridae*	70 nm	205 nm	(Peters et al., 2015)
DLP6	D1571[c]	*Myoviridae*	99 nm	144 nm x 23 nm	(Peters et al., 2017)
IME-SM1	na	*Ackermannviridae*	na*	na*	(Liu, X., et al., 2015)
IME13	Clinical	*Myoviridae*	na*	na*	(Fan et al., 2012)
IME15	Clinical	*Podoviridae*	na*	na*	(Huang et al., 2012)
Marzo	ATCC 17807[e]	*Myoviridae*	na*	na*	(Patel et al., 2022)
Mendera	ATCC 17807[e]	*Myoviridae*	na*	na*	(Garza et al., 2020)
Moby	ATCC 17807[e]	*Myoviridae*	na*	na*	(Vicary et al., 2020)
phiSMA	T39	*Myoviridae*	90 nm	90 nm	(Chang et al., 2005)
Ps15	AP143S	*Myoviridae*	85 ± 2 nm	110 nm x 17 nm	(Damnjanović et al., 2022)
Pokken	ATCC 17807[e]	*Podoviridae*	na*	na*	(Hayden et al., 2019)
S3	E539[c]	*Myoviridae*	82.92 ± 1.25 nm	136.9 ± 0.59 nm x 21.43 ± 0.0 nm	(Garcia et al., 2008)
Salva	ATCC 17807[e]	*Siphoviridae*	na*	na*	(Jefferson et al., 2021)
Sm1	na	*Myoviridae*	na	na	(Zhang and Li. 2013)
Smp14	T14	*Myoviridae*	87 nm x 77 nm	129 nm x 18 nm	(Chen et al., 2007)

Table 7: Morphology and Ultrastructure Measurements of Lytic *S. maltophilia* Phages; na, not available; *, genome announcement only; Strains: **c**, Clinical; **e**, Environmental.

Morphology of Temperate and Filamentous *S. maltophilia* Phages					
Phage	*S. maltophilia* Host Strain	Family	Ultrastructure		Reference
			Capsid	*Tail*	
DLP3	D1571[c]	*Siphoviridae*	92.8 ± 4.1 x 84.0 ± 2.8 nm	202.2 ± 5.7 nm	(Peters et al., 2020)
DLP4	D1585	*Siphoviridae*	92 nm x 63 nm	139 nm	(Peters et al., 2019)
DLP5	D1614	*Siphoviridae*	na*	na*	(Peters et al., 2018)
phiSHP1	P2[e]	*Inoviridae*	2.1 µm in length	na	(Liu et al., 2012)
phiSHP3	C31	*Siphoviridae*	na	na	(Wu et al., 2021)
phiSMA6	TC79[c]	*Inoviridae*	na	na	(Petrova et al., 2014)
phiSMA7	TC79[c]	*Inoviridae*	na	na	(Petrova et al., 2014)
phiSMA9	C5	*Inoviridae*	na	na	(Hagemann et al., 2006)
S1	CECT 4793[e]	*Siphoviridae*	61.4 ± 1.35 nm	129.2 ± 1.3 nm x 9.93 ± 0.66 nm	(Garcia et al., 2008)
S2	E999[c]	*Siphoviriae*	na	na	(Garcia et al., 2008)
S4	F227	*Siphoviridae*	na	na	(Garcia et al., 2008)
smp131	T16	*Myoviridae*	60 nm	100–120 nm x 20–30 nm	(Lee et al., 2014)

Table 8: Morphology and Ultrastructure Measurements of Temperate *S. maltophilia* Phages; na, not available; *, genome announcement only; Strains: **c**, Clinical; **e**, Environmental.

Analysis of Phage Proteins

To investigate the composition of the Bfi2 viral particle, isolated phage proteins were analyzed by SDS-PAGE. Based on the preliminary experimental data, it is difficult draw conclusions on the structural proteins of the virion. It is also important to note that the techniques used to concentrate and purify Bfi2 phage proteins may need future refinement to ensure sufficient recovery of most, if not all, phage proteins. A total of four protein bands, ranging from 8 - 86 kDa in size, were observed after visualization of the SDS-PAGE gel (Figure 8). The number of structural proteins isolated from Bfi2 is smaller than those observed for other *S. maltophilia* phages (Chang et al., 2005; Han et al., 2021; Peters et al., 2020).

Protein analysis of phage ϕSMA5 by SDS-PAGE revealed a virion composed of at least 25 proteins, with the most abundant protein being approximately 43 kDa in size (Chang et al., 2005). Analysis of DLP3 structural proteins by high-performance liquid chromatography-mass spectrometry (HPLC-MS) identified a total of 21 proteins, with the major capsid protein as the most abundant protein (33.7 kDa) isolated (Peters et al., 2020). The major capsid protein serves as the main structural component of the virion capsid (Hendrix and Johnson, 2012). Moreover, a total of nine proteins from the BUCT555 virion were identified by SDS-PAGE and ranged from 19 - 89 kDa in size (Han et al., 2021). HPLC-MS of isolated BUCT555 proteins confirmed that the most abundant structural protein (34.8 kDa) corresponded to the major capsid protein of the phage particle (Han et al., 2021).

In this thesis research, the most abundant protein of Bfi2 visualized was estimated to be approximately 12 kDa in size (Figure 8). Based on its relative abundance, it is possible that this 12 kDa protein may correspond to the phage major capsid protein of Bfi2. Yet, further research is required to more closely examine the protein composition of the Bfi2 virion.

Phage Stability in Response to Temperature and pH

The lytic activity of phages may be affected by physiological conditions such as temperature and pH. As biological agents, bacteriophages are subjected to varying microenvironments *in vivo* such that their activity and stability in a wide range of pH and temperatures may impact the outcome of phage treatments or therapeutic interventions. At the time of writing, only a single study has investigated the structural stability of an *S. maltophilia* phage in response to both temperature and pH (Han et al., 2021). Therefore, additional characterization sought to determine the stability and overall activity of Bfi2 in a range of environmental conditions.

Temperature stability experiments and statistical analyses determined that Bfi2 was stable at 30°C for up to two hours in the assayed conditions. (Figure 9a). At 50°C, Bfi2 titer decreased < 1.0 log unit (~ 8%) after two hours. The significant reduction in phage titer after incubation at 50°C suggests that Bfi2 may not be stable at this temperature. Yet, ~92% of Bfi2 virions remained active after two hours of incubation at 50ºC, which may indicate some level of structural stability at this temperature (Figure 9a). Moreover, Bfi2 became increasing unstable at 60°C and phage titer significantly decreased after 20 minutes of incubation at 60°C (Figure 9b). Compared to initial titer, Bfi2 titer decreased by > 1.5 log units (~17%) after 20 minutes of incubation at 60ºC. The rapid rate of degradation at 60ºC, where ~83% of phages remained active after 20 minutes, suggests that Bfi2 is intolerant to temperatures of 60ºC and above. Bfi2 is stable at 30°C, and based on the slow rate of phage inactivation at 50ºC, may be suitable for applications that require stability in physiological temperatures (30 - 37ºC). Furthermore, the high stability of Bfi2 in neutral and basic pH conditions, further suggest that the phage could be useful in medical applications or therapy. For example, Bfi2 is stable in temperature and pH conditions that mirror those found within the human body.

The stability of Bfi2 in response to pH was assessed and statistical analyses revealed no significant effect of pH environment on phage titer after incubation at pH 5, 7, and 9 for up two hours. Bfi2 was found to be relatively stable at the tested pH values, as phage titer remained relatively consistent in the assayed conditions. Compared to initial titer, a < 1.0 log unit reduction (~10%) in Bfi2 titer was observed after the incubation period in all pH conditions (Figure 10). Based on these results, Bfi2 could remain stable in areas that are commonly affected or associated with *S. maltophilia* infections, such as the blood (pH 7.4), respiratory tract (pH 6.6), and skin (pH 4.7 - 5.0) (Fischer and Widdicombe, 2006; Lambers et al., 2006). As briefly mentioned, *S. maltophilia* is a significant colonizer in the cystic fibrosis (CF) respiratory tract (pH 2.9 - 6.5) (Cowley et al., 2015; Parkins and Floto, 2015; Pompilio et al., 2011). Although the stability of Bfi2 has yet to be determined in conditions lower than pH 5, the acidification of the CF airways could cause therapeutic preparations of Bfi2 to become increasingly unstable. Regardless of the mode of phage application, repeated doses of Bfi2 preparations to areas of mild acidity may be able to retain sufficient therapeutic phage concentrations at the site of infection.

Until recently, only ϕSMA5 had been evaluated for its stability in response to low temperatures, where the phage was found to be stable after long-term storage at 4°C for up to 16 months (Chang et al., 2005). Interestingly, the newly isolated podovirus, BUCT598, showed stability in response to a broad range of pH conditions, stable between pH 1 - 11 and highly stable between pH 2 - 10 (Han et al., 2021). Similar to Bfi2, BUCT598 was also thermostable between 4°C - 45°C, with significant decrease in titer at 60°C and complete inactivation at 75°C (Han et al., 2021).

The stability of Bfi2 parallels those reported for three *Myoviridae* phages isolated against *P. aeruginosa* (Aghaee et al., 2021). Phages PA6, PA32, and PA45 were found to remain stable at

temperatures of 30°C - 50°C, with phage viability significantly decreasing at temperatures of 60°C and 70°C) (Aghaee et al., 2021). These phages were also stable at pH 6 - 8 but lytic activity was observed to decrease slightly at pH 5 and 9 (Aghaee et al., 2021). It should be noted that recent research has begun to assess the stability of isolated phages in response to salinity (Scarascia et al., 2018; Srichaisupakit et al., 2021). Future research on Bfi2 should characterize its stability in response to additional environmental and storage conditions.

Adsorption of Phage to Host

An important factor for the phage infection process, and production of new virions, is the initial adsorption of a phage to a host bacterial cell. At least under *in vitro* conditions, the adsorption efficiency of a phage to its host is governed by the affinity of phage receptor binding proteins (RBPs) for the bacterial surface receptor (Rakhuba et al., 2010). The affinity for a host surface receptor is a functional characteristic of phage populations and experiments aimed at determining adsorption efficiency give insight into this crucial interaction (Storms et al., 2010).

While not available for all *S. maltophilia* phages, the adsorption efficiency of Bfi2 was determined and the adsorption rate constant (*k*) was calculated. Only *S. maltophilia* phages belonging to the family *Myoviridae* have been subjected to adsorption assays (Chang et al., 2005; Chen et al., 2007; Damnjanović et al., 2022; Han et al., 2021). Of these phages, only *S. maltophilia* phage Ps15 has had its adsorption rate constant (*k*) reported (Damnjanović et al., 2022).

Adsorption assays with Bfi2 determined that ~97% of phages were bound to host cells after 15 minutes of incubation (Figure 11). This finding contrasts the long adsorption period described for ϕSMA5, where only 80% of phages attached to host cells after 80 minutes of incubation (Chang et al., 2005). Similarly, adsorption curves of phage BUCT555 revealed an adsorption efficiency of ~90% after six minutes, remaining consistent until 15 minutes after incubation (Han

et al., 2021). Moreover, it was shown that 85% of smp14 virions adsorbed to host cells after five minutes of incubation, gradually rising to 95% after 30 minutes (Chen et al., 2007). However, the adsorption efficiency of Bfi2 is lower than that of the recently isolated *S. maltophilia* phage Ps15. It was found that 90% of Ps15 virions were adsorbed to host cells after five minutes, with 98 - 99% of phages adsorbed after 10 minutes of incubation (Damnjanović et al., 2022). The adsorption efficiency of Bfi2 indicates that the phage has a high affinity for the primary receptor on its target host.

While adsorption efficiency is an inherent property of the phage, the adsorption rate constant is highly dependent on the growth condition and concentration of the bacterial host population (Storms et al., 2010). The adsorption rate constants (*k*) of phages against *S. maltophilia* and co-isolated pathogens are presented in Table 9. The adsorption rate constant (*k*) for Bfi2 was calculated to be ~2.15 ± 0.06 x 10^{-9} ml min^{-1}. This adsorption rate constant is lower than the rate constant for phage Ps15 (Damnjanović et al., 2022) (Table 9). In comparison to Ps15, Bfi2 would adsorb to host cells at a slower rate, with more time required for Bfi2 to bind an equal number of host cells.

Similar rate constants have been observed for other phages against co-isolated pathogens including *E. coli* and *P. aeruginosa* (Moldovan et al., 2007; Yu et al., 2015) (Table 9). The rate constants (*k*) of *E. coli* lambda phages were found to range on the order of 10^{-10} to 10^{-9} ml min^{-1} at 37ºC when assayed in different growth media (Moldovan et al., 2007) (Table 9). Two *P. aeruginosa* phages with interspecies and interorder infectivity, PX1 and PEf1, were found to have rate constants lower than that observed for Bfi2 (Yu et al., 2015) (Table 9). In comparison to these *P. aeruginosa* phages, Bfi2 has a higher adsorption rate constant and will adsorb to host cells at a faster rate, at least under idealized conditions.

Phage	Host Strain	Adsorption Rate Constant (k) (ml min^{-1})	Reference
Bfi2	*S. maltophilia* K279a	2.15 ± 0.06 x 10^{-9}	This Thesis
Ps15	*S. maltophilia* AP14S	9.13 x 10^{-8}	(Damnjanović et al., 2022)
λ (cI857, sam7)	*E. coli* K12 (Ymel)	9.6 x 10^{-10} - 1.56 x 10^{-9}	(Moldovan et al., 2007)
PEf1	*P. aeruginosa* PAO1	8.53 x 10^{-10}	(Yu et al., 2015)
PX1	*P. aeruginosa* PAO1	3.63 x 10^{-10}	(Yu et al., 2015)

Table 9: Adsorption Rate Constants (k) of Phages against *S. maltophilia* and Co-isolated Bacterial Pathogens.

Consideration of a phage's adsorption efficiency and adsorption rate constant are important for assessing therapeutic potential. Phage therapy applications necessitate that phages are able to reach the target pathogen in sufficient numbers and that newly produced phages are able to travel to all infected sites (Nilsson, 2019). Low adsorption efficiency and a slow adsorption rate may negatively impact the ability of a phage to properly adsorb to bacteria *in vivo* and result in titers significantly lower than expected (Nilsson, 2019). Moreover, the additional time required for phages with poor adsorption to find and replicate within a host will prolong the release of new virions, which may impact their success in therapeutic applications (Shao and Wang, 2008). Future research is required to characterize the growth kinetics of Bfi2.

Future Directions

Treatment of *S. maltophilia* Biofilms

At the time of writing, no phage against *S. maltophilia* has been investigated for its ability to remove biofilms. Phages have been shown to penetrate the biofilm matrices of pathogens such as *Enterococcus faecalis, Klebsiella pneumoniae, P. aeruginosa* and *S. aureus,* due to their production of extracellular polymeric substance (EPS)-degrading enzymes (Adnan et al., 2020; Ferriol-González and Domingo-Calap, 2020; Pei and Lamas-Samanamud, 2014; Verma et al., 2010).

Recent *in vitro* research has demonstrated the ability of phages to eliminate biofilms of closely related and co-isolated pathogens, particularly *P. aeruginosa* (Chang et al., 2019; Chegini et al., 2020; Forti et al., 2018; Waters et al., 2017). In addition, *in vivo* experiments have determined that phages can inhibit biofilm formation of *P. aeruginosa* and phage treatment of preformed *P. aeruginosa* biofilms can significantly reduce biomass (Alemayehu et al., 2012; Chang et al., 2019; Forti et al., 2018; Waters et al., 2017). Additional characterization of Bfi2 should focus on the phage's ability to inhibit biofilm formation, as well as its ability to eliminate preformed biofilms of *S. maltophilia.*

Combination Therapies

A natural progression of phage therapy may be the combination of phage with antibiotic drugs. It has been shown that antibiotics may enhance the effectiveness of phages to clear infection and in the removal of bacterial biofilms (Chegini et al., 2020; Davis et al., 2021; Lin et al., 2021; Sharahi et al., 2019; Tkhilaishvili et al., 2019; Verma et al., 2010). In the case of *P. aerguniosa*, the effect of phage application was synergistically enhanced when phages were combined with antibiotics (Chang et al., 2019, Forti et al., 2018; Henriksen et al., 2019). In comparison to individual phages, phage cocktails have shown efficacy in eliminating *P. aeruginosa* biofilms *in vitro* and *in vivo* (Forti et al., 2018).

Phage administration may result in the development of bacterial resistance to phage infection in the form of bacteriophage-insensitive mutants (BIMs) (Clokie et al., 2011; Ormälä and Jalasvuori, 2013). Phage cocktails, consisting of several phages with activity against a certain bacterial species, could reduce the probability that the pathogen will develop resistance to treatment. It is still unknown how the emergence of BIMs may impact the therapeutic outcome of phage therapy and more research is required to determine the virulence of resistant phenotypes

(Ormälä and Jalasvuori, 2013). Future research on Bfi2 should attempt to quantify the frequency of BIMs and characterize the phenotypic variations that confer resistance to phage infection.

Host Cell Surface Receptors

To date, five *S. maltophilia* phages isolated from soil have had their receptors characterized (McCutcheon et al., 2018, 2020; Peters et al., 2019, 2020). All five of these phages were found to bind the type IV pilus as the bacterial cell surface receptor (McCutcheon et al., 2018, 2020; Peters et al., 2019, 2020). As Bfi2 was isolated from soil, it may be possible that the phage binds to the type IV pilus on the surface of *S. maltophilia* K279a cells. Yet, future research is required to identify and characterize the host receptor used for Bfi2 infection.

In vivo Model Systems

As mentioned briefly, characterization of phages *in vivo* is necessary to ensure that their administration does not elicit a host immune response or cause adverse side effects. The efficacy and safety of phage administration must be demonstrated in animal models and in simulated infection environments. At this time, only two *S. maltophilia* phages, DLP3 and Sm1, have been subjected to *in vivo* experimentation (Peters et al., 2020; Zhang and Li, 2013). Phage Sm1 has been the first and only *S. maltophilia phage* to be used in a murine model, where it provided protection against *S. maltophilia* infection (Zhang and Li, 2013). The effects of Bfi2 administration should be investigated *in vivo*.

Phage Receptor Engineering and Phage-Derived Enzymes

The moderate host range of Bfi2, and the resistance of some *S. maltophilia* strains to infection, may limit its use in therapy. However, studies have attempted to circumvent the development of phage resistance and have proposed techniques to manipulate host range through engineering of phage receptor binding proteins (RBPs) (Lin et al., 2012; Yehl et al., 2019). Using

site-directed mutagenesis, T3 *E. coli* phages were engineered as part of an expanded library with high levels of diversity in phage tail fiber RBPs. It was also shown that resistance did not develop against the engineered phages over an extended period of time (Yehl et al., 2019). A study by Lin et al., 2012 showed that engineered T3 *E. coli* phages, that contained partial regions of a T7 phage tail fiber genes, had expanded host range and higher adsorption efficiency compared to wild types. These results warrant further investigation, and more research is needed to evaluate the practicality of engineering phage RBPs.

Several other areas of phage biology could be exploited as alternative treatment strategies for MDR pathogens. Phage-derived enzymes have been known to have lytic and cell wall-degrading activity. Depolymerases and endolysins have important roles in the successful infection and lysis of host bacteria by phage (Cahill and Young, 2019; Knecht et al., 2020; Loessner, 2005). Studies have identified several phage-derived enzymes and have characterized their therapeutic potential *in vitro* against *S. maltophilia* and *P. aeruginosa* (Briers et al., 2011; Chen et al., 2019; Dong et al., 2015; Liu et al., 2013; Walmagh et al., 2013). As studies by Mi et al., 2019 and Schmitz et al., 2010 have shown, the sequencing and annotation of bacterial genomes have identified possible endolysins; this approach can be used with newly isolated *S. maltophilia* strains.

VI. Conclusion

In summary, Bfi2 was found to possess several desirable characteristics that suggest this phage could be used in future therapeutic applications to control *S. maltophilia*. Although future research is required, the lytic activity, moderate host range, and anti-biofilm activity of Bfi2 indicate that the phage may be suitable for the treatment of some *S. maltophilia* infections. The *in vitro* stability of Bfi2 in response to temperature and pH conditions similar to those found *in vivo* further suggests

that this phage may be a likely candidate for use in phage therapy. Moreover, the relatively high adsorption efficiency and fast adsorption rate constant (*k*) of Bfi2 under *in vitro* conditions warrant additional research to determine the infection efficacy of the phage *in vivo*. Biological studies of the interactions between Bfi2 and *S. maltophilia* are important as they will contribute to the development of new antimicrobial strategies against infections caused by this MDR bacterial pathogen.

References

Abedon, Thomas-Abedon. 2010. Phage Therapy Pharmacology. *Curr Pharm Biotechnol*. 11: 28-47.

Ackermann. 1998. Tailed Bacteriophages: the Order Caudovirales. *Adv Virus Res*. 51: 135–201.

Ackermann, Eisenstark. 1974. The Present State of Phage Taxonomy. *Intervirology*. 3: 201-219.

Adams, Lefkowitz, King, Harrach, Harrison, Knowles, Kropinski, Krupovic, Kuhn Mushegian, Nibert, Sabanadzovic, Sanfaçon, Siddell, Simmonds, Varsani, Zerbini, Orton, Smith, Gorbalenya, Davison. 2017. 50 years of the International Committee on Taxonomy of Viruses: Progress and Prospects. *Arch Virol*. 162: 1441–1446.

Adnan, Shah, Jamal, Jalil, Andleeb, Nawaz, Pervez, Hussain, Shah, Imran. 2020. Isolation and characterization of Bacteriophage to Control Multidrug-resistant *Pseudomonas aeruginosa* Planktonic Cells and Biofilm. *Biologicals*. 63: 89–96.

Agarwal, Johnson, Imhoff, Donlan, McCarty, García, 2018. Inhaled Bacteriophage-loaded Polymeric Microparticles Ameliorate Acute Lung Infections. *Nature Biomed Eng*. 2: 841–849.

Aghaee, Khan Mirzaei, Alikhani, Mojtahedi, Maurice. 2021. Improving the Inhibitory Effect of Phages against *Pseudomonas aeruginosa* Isolated from a Burn Patient Using a Combination of Phages and Antibiotics. *Viruses*. 13: 334.

Ahern, Das, Bhowmick, Young, Gonzalez. 2014. Characterization of Novel Virulent Broad-host-range Phages of *Xylella fastidiosa* and *Xanthomonas*. *J Bacteriol*. 196: 459–471.

Akçakaya, Sargin, Hasbi Erbil, Yazici, Ari Yaylali, Mesçi, Ergin, Midilli. 2011. A Cluster of Acute-onset Postoperative Endophthalmitis Over a 1-month Period: Investigation of an Outbreak Caused by Uncommon Species. *Br J Ophthalmol*. 95: 481–484.

Al-Jasser. 2006. *Stenotrophomonas maltophilia* Resistant to Trimethoprim-sulfamethoxazole: An Increasing Problem. *Annals of Clinl Microbiol Antimicrob*. 5: 23.

Alemayehu, Casey, McAuliffe, Guinane, Martin, Shanahan, Coffey, Ross, Hill. 2012. Bacteriophages φMR299-2 and φNH-4 Can Eliminate *Pseudomonas aeruginosa* In the Murine Lung and on Cystic Fibrosis Lung Airway Cells. *mBio*. 3: e00029-12.

Alonso, Martínez. 1997. Multiple antibiotic resistance in *Stenotrophomonas maltophilia*. *Antimicrob Agents Chemother*. 41: 1140–1142.

Ambroa, Blasco, López-Causapé, Trastoy, Fernandez-García, Bleriot, Ponce-Alonso, Pacios, López, Cantón, Kidd, Bou, Oliver, Tomás. 2020. Temperate Bacteriophages (Prophages) in *Pseudomonas aeruginosa* Isolates Belonging to the International Cystic Fibrosis Clone (CC274). *Front in Microbiol*. 11: 556706.

Arvanitidou, Vayona, Spanakis, Tsakris. 2003. Occurrence and Antimicrobial Resistance of Gram-negative Bacteria Isolated in Haemodialysis Water and Dialysate of Renal Units: Results of a Greek Multicentre Study. *J App Microbiol*. 95: 180–185.

Barbolla, Catalano, Orman, Famiglietti, Vay, Smayevsky, Centrón, Piñeiro. 2004. Class 1 Integrons Increase Trimethoprim-sulfamethoxazole MICs against Epidemiologically Unrelated *Stenotrophomonas maltophilia* Isolates. *Antimicrob Agents Chemother*. 48: 666–669.

Baumrin, Piette, Micheletti. 2017. *Stenotrophomonas maltophilia*: An Emerging Multidrug-resistant Opportunistic Pathogen in the Immunocompromised Host. *BMJ Case Rep*: bcr2017221053.

Bin Abdulhak, Zimmerman, Al Beirouti, Baddour, Tleyjeh. 2009. *Stenotrophomonas maltophilia* Infectious of Intact Skin: A Systematic Review of the Literature. *Diagn Microbiol Infect Dis.* 63: 330–333.

Breijyeh, Jubeh, Karaman. 2020. Resistance of Gram-Negative Bacteria to Current Antibacterial Agents and Approaches to Resolve It. *Molecules (Basel, Switzerland)*. 25: 1340.

Briers, Walmagh, and Lavigne. 2011. Use of bacteriophage endolysin EL188 and outer membrane permeabilizers against *Pseudomonas aeruginosa*. *J Appl Microbiol.* 110: 778–785

Brives, Pourraz. 2020. Phage therapy as a Potential Solution in the Fight against AMR: Obstacles and Possible Futures. *Palgrave Commun*. 6: 100.

Brooke. 2012. *Stenotrophomonas maltophilia*: An Emerging Global Opportunistic Pathogen. *Clin Microbiol Rev.* 1: 2-41.

Brüssow, Canchaya, Hardt. 2004. Phages and the Evolution of Bacterial Pathogens: From Genomic Rearrangements to Lysogenic Conversion. *Microbiol and Molec Biol Rev.* 68: 560–602.

Boyd, Brüssow. 2002. Common Themes among Bacteriophage-encoded Virulence Factors and Diversity among the Bacteriophages Involved. *Trends Microbiol*. 10: 521-529.

Cahill, Young. 2019. Phage Lysis: Multiple Genes for Multiple Barriers. *Adv Virus Res.* 103: 33–70.

Campbell. 2003. The Future of Bacteriophage Biology. *Nature Rev Genetics.* 4: 471–477.

Cantón, Valdezate, Vindel, Sánchez Del Saz., Maíz, Baquero. 2003. Antimicrobial Susceptibility Profile of Molecular Typed Cystic Fibrosis *Stenotrophomonas maltophilia* Isolates and Differences with Noncystic Fibrosis Isolates. *Pediatr Pulmonol.* 35: 99–107.

Casjens. 2003. Prophages and Bacterial Genomics: What Have We Learned So Far? *Molec Microbiol*. 49: 277-300.

Chang, Chen, Lin, Shen, Chang, Tseng, Weng. 2005. Isolation and Characterization of Novel Giant *Stenotrophomonas maltophilia* Phage phiSMA5. *Appl Environ Microbiol*. 71: 1387-1393.

Chang, Chen, Chang C., Lee, Wu. 2004. Contribution of Integrons, and SmeABC and SmeDEF Efflux Pumps to Multidrug Resistance in Clinical Isolates of *Stenotrophomonas maltophilia*. *Antimicrob Chemother*. 53: 518–521.

Chang, Tsai, Huang, Chung, Yang. 2011. SmQnrR, a DeoR-type Transcriptional Regulator, Negatively Regulates the Expression of Sm*qnr* and Sm*tcrA* in *Stenotrophomonas maltophilia*. *J Antimicrob Chemother*. 66L: 1024–1028.

Chang, Lin, Chen, Hsueh. 2015. Update on Infections Caused by *Stenotrophomonas maltophilia* with Particular Attention to Resistance Mechanisms and Therapeutic Options. *Front in Microbiol.* 6: 893.

Chang, Das, Manos, Elizabeth Kutter, Morales, Chan. 2019. Bacteriophage PEV20 and Ciprofloxacin Combination Treatment Enhances Removal of *Pseudomonas aeruginosa* Biofilm Isolated from Cystic Fibrosis and Wound Patients. *AAPS J*. 21: 49.

Chanishvili. 2012. Phage Therapy—History from Twort and d'Herelle Through Soviet Experience to Current Approaches. *Adv in Virus Res*. 83: 3–40.

Chanishvili. 2016. Bacteriophages as Therapeutic and Prophylactic Means: Summary of the Soviet and Post-Soviet Experiences. *Curr Drug Deliv.* 13: 309–323.

Chegini, Khoshbayan, Taati, Moghadam, Farahani, Jazireian, Shariati. 2020. Bacteriophage Therapy against *Pseudomonas aeruginosa* Biofilms: a Review. *Ann Clin Microbiol Antimicrob.* 19: 45.

Chen, Lin, Lin J., Chang, Tseng, Weng. 2007. Characterization of a Novel T4-type *Stenotrophomonas maltophilia* Virulent Phage Smp14. *Arch Microbiol.* 188: 191–197.

Chen, Wang, Sun, Chen, Lai, Wu, Tan. 2010. Endophthalmitis Caused by *Stenotrophomonas maltophilia*. *Ophthalmic Surg Lasers Imaging.* 41: e555–e561.

Chibani, Farr, Klama, Dietrich, Liesegang. 2019. Classifying the Unclassified: A Phage Classification Method. *Viruses*. 11: 195.

Chung, Kim, Hong, Hong, Lee, Chong. 2015. The *sul1* Gene in *Stenotrophomonas maltophilia* with High-level Resistance to Trimethoprim/sulfamethoxazole. *Ann Lab Med.* 35: 246–249.

Clementz, Bednarsk, Raetz. 1996. Function of the htrB High Temperature Requirement Gene of *Escherichia coli* in the Acylation of Lipid A: HtrB Catalyzed Incorporation of Laurate. *J Biol Chem*. 271: 12095–12102.

Clokie, Millard, Letarov, Heaphy. 2011. Phages in Nature. *Bacteriophage.* 1: 31–45.

Cowley, Kopf, LaRiviere, Ziebis, Newman. 2015. Pediatric Cystic Fibrosis Sputum can be Chemically Dynamic, Anoxic, and Extremely Reduced due to Hydrogen Sulfide Formation. *mBio*. 6: e00767-e00815.

Crossman, Gould, Dow, Vernikos, Okazaki, Sebaihia, Saunders, Arrowsmith, Carver, Peters, Adlem, Kerhornou, Lord, Murphy, Seeger, Squares, Rutter, Quail, Rajandream, Harris, Churcher, Bentley, Parkhill, Thomson, Avison. 2008. The Complete Genome, Comparative and Functional Analysis of *Stenotrophomonas maltophilia* reveals an Organism Heavily Shielded by Drug Resistance Determinants. *Genome Biol*. 9: R74.

Damnjanović, Vázquez-Campos, Elliott, Willcox, Bridge. 2022. Characterization of Bacteriophage vB_SmaM_Ps15 Infective to *Stenotrophomonas maltophilia* Clinical Ocular Isolates. *Viruses*. 14: 709.

Danis-Wlodarczyk, Olszak, Arabski, Wasik, Majkowska-Skrobek, Augustyniak, Gula, Briers, Jang, Vandenheuvel, Duda, Lavigne, Drulis-Kawa. 2015. Characterization of the Newly Isolated Lytic Bacteriophages KTN6 and KT28 and Their Efficacy against *Pseudomonas aeruginosa* Biofilm. *PloS one*. 10: e0127603.

Davis, McCutcheon, Dennis. 2021. Aztreonam Lysine Increases the Activity of Phages E79 and phiKZ against *Pseudomonas aeruginosa* PA01. *Microorganisms (Basel)*. 9: 152.

del Toro, Rodríguez-Bano, Herrero, Rivero, García-Ordoñez, Corzo, Pérez-Cano, Grupo Andaluz para el Estudio de las Enfermedades Infecciosast. 2002. Clinical Epidemiology of *Stenotrophomonas maltophilia* Colonization and Infection: a Multicenter Study. *Medicine (Baltimore).* 81: 228–239.

de Melo, da Mata Gomes, Melo, Ardisson-Araújo, de Vargas, Ely, Kitajima, Ribeiro, Wolff. 2019. Characterization of a Bacteriophage with Broad Host Range against Strains of *Pseudomonas aeruginosa* Isolated from Domestic Animals. *BMC Microbiol.* 19: 134.

Demuth, Neve, Witzel. 1993. Direct Electron Microscopy Study on the Morphological Diversity of Bacteriophage Populations in Lake Plusssee. *Appl Environ Microbiol.* 59: 3378–3384.

DeNegre, Ndeffo Mbah, Myers, Fefferman. 2019. Emergence of Antibiotic Resistance in Immunocompromised Host Populations: A Case Study of Emerging Antibiotic Resistant *tuberculosis* in AIDS Patients. *PloS one*. 14: e0212969.

Denton, Kerr. 1998. Microbiological and Clinical Aspects of Infection Associated with *Stenotrophomonas maltophilia*. *Clin Microbiol Rev*. 11: 57–80.

de Oliveira, Forde, Kidd TJ, Harris, Schembri, Beatson, Paterson, Walker. 2020. Antimicrobial Resistance in ESKAPE Pathogens. *Clin Microbiol Rev*. 33: e00181-19.

Domingues, da Silva, Nielsen. 2012. Integrons: Vehicles and Pathways for Horizontal Dissemination in Bacteria. *Mob Genetic Elements*. 2: 211-223.

Dong, Zhu, Chen, Ye, Huang. 2015. Antibacterial Activity of *Stenotrophomonas maltophilia* Endolysin P28 against both Gram-positive and Gram-negative Bacteria. *Front in Microbiol*. 6: 1299.

Donlan. 2002. Biofilms: Microbial Life on Surfaces. *Emerg Infect Dis*. 8: 881-90.

Downhour, Petersen, Krueger, Tangella, Nix. 2002. Severe Cellulitis/myositis Caused by *Stenotrophomonas maltophilia*. *Ann Pharmacother*. 36: 63– 66.

Duplessis, Biswas, Hanisch, Perkins, Henry, Quinones, Wolfe, Estrella, Hamilton. 2018. Refractory *Pseudomonas* Bacteremia in a 2-Year-Old Sterilized by Bacteriophage Therapy. *J Pediatric Infect Dis Soc*. 7: 253-256.

Ewig, Soler, Gonzalez, Celis, El-Ebiary, Torres. 2000. Evaluation of Antimicrobial Treatment in Mechanically Ventilated Patients with Severe Chronic Obstructive Pulmonary Disease Exacerbations. *Crit Care Med*. 28: 692–697.

Falagas, Kastoris, Vouloumanou, Dimopoulos. 2009. Community-acquired *Stenotrophomonas maltophilia* Infections: A Systematic Review. *Eur J Clin Microbiol Infect Dis*. 28: 719-30.

Fan, Huang, Mi, Yin, Wang, Fan, H., Zhang, An, Chen, Tong. 2012. Complete Genome Sequence of IME13, a *Stenotrophomonas maltophilia* Bacteriophage with Large Burst Size and Unique Plaque Polymorphism. *J Virol*. 86: 11392–11393.

Fernandes, São-José. 2018. Enzymes and Mechanisms Employed by Tailed Bacteriophages to Breach the Bacterial Cell Barriers. *Viruses*. 10: 396.

Ferriol-González, Domingo-Calap. 2020. Phages for Biofilm Removal. *Antibiotics (Basel, Switzerland)*. 9: 268.

Fischer, Widdicombe. 2006. Mechanisms of Acid and Base Secretion by the Airway Epithelium. *J Membrane Biology*. 211: 139–150.

Fish, Kutter, Bryan, Wheat, Kuhl. 2018. Resolving Digital Staphylococcal Osteomyelitis Using Bacteriophage-A Case Report. *Antibiotics (Basel, Switzerland)*. 7: 87.

Fish, Kutter, Wheat, Blasdel, Kutateladze, Kuhl. 2018b. Compassionate Use of Bacteriophage Therapy for Foot Ulcer Treatment as an Effective Step for Moving Toward Clinical Trials. *Methods Mol Biol*. 1693: 159-170.

Flemming, Wingender, Griegbe, Mayer. 2000. Physico-chemical Properties of Biofilms. *In: Evans LV, editor. Biofilms: recent advances in their study and control. Amsterdam: Harwood Academic Publishers:* 19–34.

Flores-Treviño, Gutiérrez-Ferman, Morfín-Otero, Rodríguez-Noriega, Estrada-Rivadeneyra, Rivas-Morales, Llaca-Díaz, Camacho-Ortíz, Mendoza-Olazarán, Garza-González. 2014. *Stenotrophomonas maltophilia* in Mexico: Antimicrobial Resistance, Biofilm Formation and Clonal Diversity. *J Med Microbiol*. 63: 1524-1530.

Forti, Roach, Cafora, Pasini, Horner, Fiscarelli, Rossitto, Cariani, Briani, Debarbieux, Ghisotti. 2018. Design of a Broad-Range Bacteriophage Cocktail That Reduces *Pseudomonas aeruginosa* Biofilms and Treats Acute Infections in Two Animal Models. *Antimicrob Agents Chemother*. 62: e02573-17.

Fothergill, Walshaw, Winstanley. 2012. Transmissible Strains of *Pseudomonas aeruginosa* in Cystic Fibrosis Lung Infections. *Eur Respir J.* 40: 227–238.

Fujita, Yamadori, Xu, Hojo, Negayama, Miyawaki, Yamaji, Takahara. 1996. Clinical Features of *Stenotrophomonas maltophilia* Pneumonia in Immunocompromised Patients. *Respir Med.* 90: 35–38.

Gales, Jones, Forward, Liñares, Sader, Verhoef. 2001. Emerging Importance of Multidrug-resistant *Acinetobacter* Species and *Stenotrophomonas maltophilia* as Pathogens in Seriously Ill Patients: Geographic Patterns, Epidemiological Features, and Trends in the SENTRY Antimicrobial Surveillance Program (1997-1999). *Clin Infect Dis.* 32: S104–S113.

Gallagher, Phan, Oliver, Chase, England, Wandro, Hendrickson, Riedel, Whiteson. 2019. Cystic Fibrosis-associated *Stenotrophomonas maltophilia* Strain-specific Adaptations and Responses to pH. *J Bacteriol*. 201: e00478-e00518.

Gao, Lyu, Li. 2017. Trends in Drug Resistance of *Acinetobacter baumannii* over a 10-year Period: Nationwide Data from the China Surveillance of Antimicrobial Resistance Program. *Chinese Med J.* 130: 659–664.

García-León, Ruiz de la Alegría Puig, García de la Fuente, Martínez-Martínez, Martínez, Sánchez. 2015. High-level Quinolone Resistance is Associated to the Overexpression of SmeVWX in *Stenotrophomonas maltophilia* Clinical Isolates. *Clin Microbiol Infect*. 21: 464–467.

García-León, Salgado, Oliveros, Sanchez, Martinez. 2014. Interplay between Intrinsic and Acquired Resistance to Quinolones in *Stenotrophomonas maltophilia*. *Environ Microbiol*. 16: 1282–1296.

García, Monjardín, Martín, Madera, Soberón, Garcia, Meana, Suárez. 2008. Isolation of New *Stenotrophomonas* Bacteriophages and Genomic Characterization of Temperate Phage S1. *Appl and Environ Microbiol.* 74: 7552-7560.

Garza, Newkirk, Moreland, Gonzalez, Liu, Ramsey, Leavitt. 2020. Complete Genome Sequence of *Stenotrophomonas* Phage Mendera. *Microbiol Resour Announc*. 9: e01411-19.

Gill, Hyman. 2010. Phage Choice, Isolation, and Preparation for Phage Therapy. *Curr Pharm Biotechnol*. 11: 2-14.

Górski, Międzybrodzki, Łobocka, Głowacka-Rutkowska, Bednarek, Borysowski, Jończyk-Matysiak, Łusiak-Szelachowska, Weber-Dąbrowska, Bagińska, Letkiewicz, Dąbrowska, Scheres. 2018. Phage therapy: What Have We Learned? *Viruses.* 10: 288.

Gülmez, Hasçelik. 2005. *Stenotrophomonas maltophilia*: Antimicrobial Resistance and Molecular Typing of an Emerging Pathogen in a Turkish University Hospital. *Clin Microbiol Infect.* 11: 880–886.

Hagemann, Hasse, Berg. 2006. Detection of a Phage Genome Carrying a Zonula Occludens like Toxin Gene (zot) in Clinical Isolates of *Stenotrophomonas maltophilia*. *Arch Microbiol.* 185: 449–458.

Hall, Collins. 1995. Mobile Gene Cassettes and Integrons: Capture and Spread of Genes by Site-specific Recombination. *Molec Microbiol.* 15: 593-600.

Han, He, Fan, Song, An, Li, Tong. 2022. Characterization and Genome Analysis of a Novel *Stenotrophomonas maltophilia* Bacteriophage BUCT598 with Extreme pH Resistance. *Virus Res*. 314: 198751.

Han, Hu, An, Song, Fan, Tong. 2021. Biochemical and Genomic Characterization of a Novel Bacteriophage BUCT555 Lysing *Stenotrophomonas maltophilia*. *Virus Res*. 301: 198465.

Häusler. 2006. News Feature: Bug Killers. *Nat. Med*. 12: 600–601.

Hayden, Martinez, Moreland, Liu, Gonzalez, Gill, Ramsey. 2019. Complete Genome Sequence of *Stenotrophomonas* Phage Pokken. *Microbiol Resour Announc*. 8: e01095-e01119.

Henriksen, Rørbo, Rybtke, Martinet, Tolker-Nielsen, Høiby, Middelboe, Ciofu. 2019. *P. aeruginosa* Flow-cell Biofilms are Enhanced by Repeated Phage Treatments but can be Eradicated by Phage-ciprofloxacin Combination. *Pathog Dis*. 77: ftz011.

Ho, Juurlink. 2011. Considerations When Prescribing Trimethoprim-sulfamethoxazole. *CMAJ*: *Can Med Assoc J*. 183: 1851–1858.

Hotta, Matsumura, Kato, Nakano, Yunoki, Yamamoto. 2014. Risk factors and outcomes of *Stenotrophomonas maltophilia* bacteraemia: a comparison with bacteraemia caused by *Pseudomonas aeruginosa* and *Acinetobacter* species. *PLoS one*. 9: e112208.

Huang, Fan, Pei, Fan, Zhang, An, Mi, Shi, Tong. 2012. Complete Genome Sequence of IME15, the First T7-Like Bacteriophage Lytic to Pan-antibiotic-resistant S*tenotrophomonas maltophilia*. *J Virol*. 86: 13839–13840.

Huang, Hu, Lin, Huang, H., Yang. 2015. The Contribution of Class 1 Integron to Antimicrobial Resistance in *Stenotrophomonas maltophilia*. *Microb Drug Res.* 21: 9–96.

Huang, Lin, Hu, Lin, Chung, Yang. 2010. AmpN-AmpG Operon is Essential for Expression of L1 and L2 Beta-lactamases in *Stenotrophomonas maltophilia*. *Antimicrob Agents Chemother*. 54: 2583–2589.

Hu, Chang, Ye, Wang, Shao, Shi, Li, Li, J. 2011. *Stenotrophomonas maltophilia* Resistance to Trimethoprim/sulfamethoxazole Mediated by Acquisition of *sul* and *dfrA* Genes in a Plasmid-mediated Class 1 Integron. *Int J Antimicrob Agents*. 37: 230-234.

Hyman. 2019. Phages for Phage Therapy: Isolation, Characterization, and Host Range Breadth. *Pharmaceuticals (Basel)*. 12: 35.

Hyman, Abedon. 2009. Practical Methods for Determining Phage Growth Parameters. *Methods Mol Biol*. 501: 175-202.

Hyman, Abedon. 2010. Bacteriophage Host Range and Bacterial Resistance. *Adv Appl Microbiol.* 70: 217–248.

Jang, Wang, Wang, Liu, Liu. 1992. *Xanthomonas maltophilia* Bacteremia: An Analysis of 32 Cases. *J Formos Med Assoc.* 91: 1170–1179.

Jefferson, Yao, Clark, Le, Gonzalez, Liu, Burrowes. 2021. Complete Genome Sequence of *Stenotrophomonas maltophilia* Siphophage Salva. *Microbiol Resour Announc*. 10: e00083-e00121.

Johansen, Moskowitz, Ciofu, Pressler, and Høiby. 2008. Spread of Colistin Resistant Non-mucoid *Pseudomonas aeruginosa* among Chronically Infected Danish Cystic Fibrosis Patients. *J Cyst Fibro.* 7: 391–397.

Kalghatgi, Spina, Costello, Liesa, Morones-Ramirez, Slomovic, Molina, Shirihai, Collins. 2013. Bactericidal Antibiotics Induce Mitochondrial Dysfunction and Oxidative Damage in Mammalian Cells. *Sci Transl Med*. 5: 192ra85.

Kawahara, Tsukano, Watanabe, Lindner, Matsuura. 2002. Modification of the Structure and Activity of Lipid A in *Yersinia pestis* Lipopolysaccharide by Growth Temperature. *Infect Immun.* 70: 4092–4098.

Khan Mirzaei, Nilsson. 2015. Isolation of Phages for Phage Therapy: a Comparison of Spot Tests and Efficiency of Plating Analyses for Determination of Host Range and Efficacy. *PloS one*. 10: e0118557.

Khawaldeh, Morales, Dillon, Alavidze, Ginn, Thomas, Chapman, Dublanchet, Smithyman, Iredell. 2011. Bacteriophage Therapy for Refractory *Pseudomonas aeruginosa* Urinary Tract Infection. *J Med Microbiol*. 60: 1697-1700.

Kidd, Ramsa, Hu, Marks, Wainwright, Bye. 2013. Shared *Pseudomonas aeruginosa* Genotypes Are Common in Australian Cystic Fibrosis Centres. *Eur Respir J.* 41: 1091–1100.

Kidd, Canton, Ekkelenkamp, Johansen, Gilligan, LiPuma, Bell, Elborn, Flume, VanDevanter, Waters. 2018. Defining Antimicrobial Resistance in Cystic Fibrosis. *J Cyst Fibros*. 17: 696–704.

Kim, Kim, Y., Ahn, Jeong, Ku, Choi, Yeom, Song. 2019. Risk factors for Mortality in Patients with *Stenotrophomonas maltophilia* Bacteremia and Clinical Impact of Quinolone–resistant Strains. *BMC Infect Dis.* 19: 754.

Knecht, Veljkovic, Fieseler. 2020. Diversity and Function of Phage Encoded Depolymerases. *Front in Microbiol*. 10: 2949.

Kropinski, Mazzocco, Waddell, Lingohr, Johnson. 2009. Enumeration of Bacteriophages by Double Agar Overlay Plaque Assay. *Methods Mol Biol*. 501: 69-76.

Kutateladze. 2015. Experience of the Eliava Institute in Bacteriophage Therapy. *Virol Sin*. 30: 80-81.

Kutateladze, Adamia. 2008. Phage Therapy Experience at the Eliava Institute. *Med Mal Infect*. 38: 426-430.

Lai, Chi, Chen, Chen, Lai, Fung. Yu, Wong, Liu. 2004. Clinical characteristics and Prognostic Factors of Patients with *Stenotrophomonas maltophilia* Bacteremia. *J Microbiol Immunol Infect*. 37: 350–358.

Lai, Wong, Chin, Huang, Lin, Chen, Yu, Liu. 2006. Central Venous Catheter-related *Stenotrophomonas maltophilia* Bacteraemia and Associated Relapsing Bacteraemia in Haematology and Oncology Patients. *Clin Microbiol Infect*. 12: 986–999.

Lambers, Piessens, Bloem, Pronk, Finkel. 2006. Natural Skin Surface pH is on Average below 5, which is Beneficial for its Resident Flora. *Int J Cosmet Sci*. 5: 359-70.

Landrum, Conger, Forgione. 2005. Trimethoprim-sulfamethoxazole in the Treatment of *Stenotrophomonas maltophilia* Osteomyelitis. *Clin Infect Dis.* 40: 1551–1552.

Lee, Tseng, Chang, Lin, Weng. 2014. Genomic Sequence of Temperate Phage Smp131 of *Stenotrophomonas maltophilia* That Has Similar Prophages in *Xanthomonads*. *BMC Microbiol.* 14: 17.

Levison, Levison, J. 2009. Pharmacokinetics and Pharmacodynamics of Antibacterial Agents. *Infect Dis Clin North Am*. 23: 791-815, vii.

Li, Zhang, McKay, Poole. 2003. Role of the Acetyltransferase AAC(6')-Iz Modifying Enzyme in Aminoglycoside Resistance in *Stenotrophomonas maltophilia*. *Antimicrob Chemother*. 51: 803-811.

Lin, Huang, Chen, Chang, Yang. 2015. The SmeYZ Efflux Pump of *Stenotrophomonas maltophilia* Contributes to Drug Resistance, Virulence-Related Characteristics, and Virulence in Mice. *Antimicrob Agents and Chemother*. 59: 4067–4073.

Lin, Huang, Liou, Chang, Yang. 2014. MacABCsm, an ABC-type Tripartite Efflux Pump of *Stenotrophomonas maltophilia* Involved in Drug Resistance, Oxidative and

Envelope Stress Tolerances and Biofilm Formation. A*ntimicrob Chemother*. 69: 3221–3226.

Lin, Lo, Tseng, Chang, Lin, Chen. 2012. A T3 and T7 Recombinant Phage Acquires Efficient Adsorption and a Broader Host Range. *PloS one*. 7: e30954.

Lin, Quan, Chang, Chow, Wang, Li, Morales, Britton, Kutter, Li J, Chan. 2021. Synergistic Activity of Phage PEV20-ciprofloxacin Combination Powder Formulation-A Proof-of-Principle Study in a *P. aeruginosa* Lung Infection Model. *Eur J Pharm Biopharm*. 158: 166-171.

Liu, Chen, Zheng, Huang. 2013. Characterization of Maltocin P28, a Novel Phage Tail-like Bacteriocin from *Stenotrophomonas maltophilia*. *Appl Environ Microbiol*. 79: 5593–5600.

Liu, Liu Q., Shen, Huang. 2012. Isolation and Characterization of a Novel Filamentous Phage from *Stenotrophomonas maltophilia*. *Arch Virol*. 157: 1643–1650.

Loessner. 2005. Bacteriophage Endolysins--Current State of Research and Applications. *Curr Opin Microbiol*. 8: 480-7.

Lunde, Aastveit, Blatny, Nes. 2005. Effects of Diverse Environmental Conditions on {phi} LC3 Prophage Stability in *Lactococcus lactis*. *Appl Environ Microbiol*. 71: 721–727.

Lu, Breidt. 2015. *Escherichia coli* O157:H7 Bacteriophage Φ241 Isolated from an Industrial Cucumber Fermentation at High Acidity and Salinity. *Front in Microbiol.* 6: 67.

Marquez, Newkirk, Moreland, Gonzalez, Liu, Ramsey. 2019. Complete Genome Sequence of *Stenotrophomonas maltophilia* Podophage Ponderosa. *Microbiol Resour Announc*. 8: e01032-19.

Matos, Lapaque, Rigottier-Gois, Debarbieux, Meylheuc, Gonzalez-Zorn, Repoila, Lopes, Serror. 2013. *Enterococcus faecalis* Prophage Dynamics and Contributions to Pathogenic Traits. *PLoS Genetics*. 9: e1003539.

Matsuura. 2013. Structural Modifications of Bacterial Lipopolysaccharide that Facilitate Gram-negative Bacteria Evasion of Host Innate Immunity. *Front in Immunol*. 4:109.

McCallin, Sacher, Zheng, Chan. 2019. Current State of Compassionate Phage Therapy. *Viruses.* 11: 343.

McCutcheon, Dennis. 2021. The Potential of Phage Therapy against the Emerging Opportunistic Pathogen *Stenotrophomonas maltophilia*. *Viruses.* 13: 1057.

McCutcheon, Lin, Dennis. 2020. Isolation and Characterization of the Novel Bacteriophage AXL3 against *Stenotrophomonas maltophilia*. *Int J of Molec Sci.* 21: 6338.

McCutcheon, Peters, Dennis. 2018. Identification and Characterization of Type IV Pili as the Cellular Receptor of Broad Host Range *Stenotrophomonas maltophilia* Bacteriophages DLP1 and DLP2. *Viruses*. 10: 338.

Memish, Shibl, Kambal, Ohaly, Ishaq, Livermore. 2012. Antimicrobial Resistance Among Non-fermenting Gram-negative Bacteria in Saudi Arabia. *J. Antimicrob. Chemother*. 67: 1701–1705.

Mesaros Nordmann, Plésiat, Roussel-Delvallez, Van Eldere, Glupczynski, Van Laethem, Jacobs, Lebecque, Malfroot, Tulkens, Van Bambeke. 2007. *Pseudomonas aeruginosa*: Resistance and Therapeutic Options at the Turn of the New Millennium. *Clin Microbiol Infect*. 13: 560-578.

Mi, Liu, Wang, He, Gao, Xing, Huang, Fan, Zhang, Yu, Mi, Z., Tong, Bai, Han. 2019. Identification of a lytic *Pseudomonas aeruginosa* Phage Depolymerase and its Anti-biofilm Effect and Bactericidal Contribution to Serum. *Virus Genes*. 55: 394–405.

Micozzi, Venditti, Monaco, Friedrich, Taglietti, Santilli, Martino. 2000. Bacteremia Due to *Stenotrophomonas maltophilia* in Patients with Hematologic Malignancies. *Clin Infect Dis*. 31: 705–711.

Moldovan, Chapman-McQuiston, Wu. 2007. On Kinetics of Phage Adsorption. *Biophys J*. 93: 303-315.

Moore, Millar, Courtney, Elborn. 2003. Development of a Gram-negative Selective Agar (GNSA) for the Detection of Gram-negative Microflora in Sputa in Patients with Cystic Fibrosis. *J Appl Microbiol*. 95: 160–166.

Ng, Tai, Chang, Stick, Kicic. 2021. Overcoming Challenges to Make Bacteriophage Therapy Standard Clinical Treatment Practice for Cystic Fibrosis. *Front in Microbiol.* 11: 593988.

Nguyen, Muder. 1994. Meningitis Due to *Xanthomonas maltophilia*: Case Report and Review. *Clin Infect Dis*. 19: 325–326.

Nilsson. 2019. Pharmacological Limitations of Phage Therapy. *Upsala J Med Sci*. 124: 218–227.

Nseir, Di Pompeo, Cavestri, Jozefowicz, Nyunga, Soubrier, Roussel-Delvallez, Saulnier, Mathieu, Durocher. 2006. Multiple-drug-resistant Bacteria in Patients with Severe Acute Exacerbation of Chronic Obstructive Pulmonary Disease: Prevalence, Risk Factors, and Outcome. *Crit Care Med*. 34: 2959–2966.

Okazaki, Avison. 2007. Aph (3′)-IIc, an Aminoglycoside Resistance Determinant from *Stenotrophomonas maltophilia*. *Antimicrob Agents Chemother*. 51: 359–360.

Okazaki, Avison. 2008. Induction of L1 and L2 Beta-lactamase Production in *Stenotrophomonas maltophilia* is Dependent on an AmpR-type Regulator. *Antimicrob Agents Chemother*. 52: 1525–1528.

Ormälä, Jalasvuori. 2013. Phage therapy: Should Bacterial Resistance to Phages be a Concern, Even in the Long run? *Bacteriophage*. 3: e24219.

Palleroni, Bradbury. 1993. *Stenotrophomonas*, a New Bacterial Genus for *Xanthomonas maltophilia* (Hugh, 1980) Swings et al. 1983. *Int J Syst Bacteriol.* 43: 606–609.

Papadakis, Vartivarian, Vassilaki, Anaissie. 1995. *Stenotrophomonas maltophilia:* An Unusual Case of Biliary Sepsis. *Clin Infect Dis*. 21: 1032–1034.

Parkins, Floto. 2015. Emerging Bacterial Pathogens and Changing Concepts of Bacterial Pathogenesis in Cystic Fibrosis. *J Cyst Fibros*. 14: 293-304.

Parkins, Glezerson, Sibley, Sibley, Duong, Purighalla, Mody, Workentine, Storey, Surette, Rabin. 2014. Twenty-five-year Outbreak of *Pseudomonas aeruginosa* Infecting Individuals with Cystic Fibrosis: Identification of the Prairie Epidemic Strain. *J Clin Microbiol.* 52: 1127–1135.

Parracho, Burrowes, Enright, McConville, Harper. 2012. The Role of Regulated Clinical Trials in the Development of Bacteriophage Therapeutics. *J Molec Genetic Med: an Int J Biomed Res*. 6: 279–286.

Patel, Godoy, Clark, Burrowes, Young, Liu. 2022. Complete Genome Sequence of *Stenotrophomonas maltophilia* Myophage Marzo. *Microbiol Resour Announc.* 11: e0120221.

Pei, Lamas-Samanamud. 2014. Inhibition of Biofilm Formation by T7 Bacteriophages Producing Quorum-quenching Enzymes. *Appl Environ Microbiol*. 80: 5340–5348.

Petrova, Shcherbatova, Kurakov, Mindlin. 2013. Genomic Characterization and Integrative Properties of phiSMA6 and phiSMA7, Two Novel Filamentous Bacteriophages of *Stenotrophomonas maltophilia*. *Arch Virol.* 159: 1293-1303.

Peters, Dennis. 2018. Complete Genome Sequence of Temperate *Stenotrophomonas maltophilia* Bacteriophage DLP5. *Genome announ.* 6: e00073-18.

Peters, Lynch, Stothard, Dennis. 2015. The Isolation and Characterization of Two *Stenotrophomonas maltophilia* Bacteriophages Capable of Cross-taxonomic Order Infectivity. *BMC genomics*. 16: 664.

Peters, McCutcheon, Dennis. 2020. Characterization of Novel Broad-Host-Range Bacteriophage DLP3 Specific to *Stenotrophomonas maltophilia* as a Potential Therapeutic Agent. *Front in Microbiol.* 11: 1358.

Peters. McCutcheon. Stothard. Dennis. 2019. Novel *Stenotrophomonas maltophilia* Temperate Phage DLP4 is Capable of Lysogenic Conversion. *BMC Genomics.* 20: 300.

Peters, Stothard, Dennis. 2017. The Isolation and Characterization of *Stenotrophomonas maltophilia* T4-like Bacteriophage DLP6. *PloS one*. 12; 3: e0173341.

Pompilio, Pomponio, Crocetta, Gherardi, Verginelli, Fiscarelli, Dicuonzo, Savini, D'Antonio, Di Bonaventura. 2011. Phenotypic and Genotypic Characterization of *Stenotrophomonas maltophilia* Isolates from Patients with Cystic Fibrosis: Genome Diversity, Biofilm Formation, and Virulence. *BMC Microbiol.* 11: 159.

Principi, Silvestri, Esposito. 2019. Advantages and Limitations of Bacteriophages for the Treatment of Bacterial Infections. *Front Pharmacol*. 10: 513.

Rajan, Saiman. 2002. Pulmonary Infections in Patients with Cystic Fibrosis. *Sem in Respir Infect.* 17: 47–56.

Rakhuba, Kolomiets, Dey, Novik. 2010. Bacteriophage Receptors, Mechanisms of Phage Adsorption and Penetration into Host Cell. *Polish J Microbiol*. 59: 145–155.

Rattanaumpawan, Ussavasodhi, Kiratisin, Aswapokee. 2013. Epidemiology of Bacteremia Caused by Uncommon Non-fermentative Gram-negative Bacteria. *BMC Infect Dis*. 13: 167.

Rhee, Choi, Choi, Peck, Ko. 2013. Distinct Groups and Antimicrobial Resistance of Clinical *Stenotrophomonas maltophilia* Complex Isolates from Korea. *J Med Microbiol.* 62: 748–753.

Rhoads, Wolcott, Kuskowski, Wolcott, Ward, Sulakvelidze. 2009. Bacteriophage Therapy of Venous Leg Ulcers in Humans: Results of a Phase I Safety Trial. *J Wound Care*. 18: 237–243.

Ross, Ward, Hyman. 2016. More Is Better: Selecting for Broad Host Range Bacteriophages. *Front in Microbiol*. 7: 1352.

Ruppé, Woerther, Barbier. 2015. Mechanisms of Antimicrobial Resistance in Gram-negative Bacilli. *Ann Intensiv Care.* 5: 61.

Sader, Jones. 2005. Antimicrobial Susceptibility of Uncommonly Isolated Non-enteric Gram-negative Bacilli. *Int J Antimicrob Agents* 25: 95–109.

Sader, Farrell, Flamm, Jones. 2014. Antimicrobial Susceptibility of Gram-negative Organisms Isolated from Patients Hospitalised with Pneumonia in US and European Hospitals: Results from the SENTRY Antimicrobial Surveillance Program, 2009-2012. *Int J Antimicrob Agents*. 43: 328–334.

Saiman, Chen, Gabriel, Knirsch. 2002. Synergistic Activities of Macrolide Antibiotics against *Pseudomonas aeruginosa, Burkholderia cepacia, Stenotrophomonas maltophilia,* and *Alcaligenes xylosoxidans,* Isolated From Patients with Cystic Fibrosis. *Antimicrob Agents Chemother*. 46: 1105–1107.

Sakhnini, Weissmann, Oren. 2002. Fulminant *Stenotrophomonas maltophilia* Soft Tissue Infection in Immunocompromised Patients: An Outbreak Transmitted via Tap Water. *Am J Med Sci*. 323: 269-272.

Salsgiver, Fink, Knapp, LiPuma, Olivier, Marshall, Saiman. 2016. Changing Epidemiology of the Respiratory Bacteriology of Patients with Cystic Fibrosis. *Chest*. 149: 390–400.

Salunkhe, Smart, Morgan, Panagea, Walshaw, Hart, Geffers, Tümmler, Winstanley. 2005. A Cystic Fibrosis Epidemic Strain of *Pseudomonas aeruginosa* Displays Enhanced Virulence and Antimicrobial Resistance. *J Bacteriol*. 187: 4908-4920.

Sánchez. 2015. Antibiotic Resistance in the Opportunistic Pathogen *Stenotrophomonas maltophilia*. *Front in Microbiol*. 6: 658–658.

San Gabriel, Zhou, Tabibi, Chen, Trauzzi, Saiman. 2004. Antimicrobial Susceptibility and Synergy Studies of *Stenotrophomonas maltophilia* Isolates from Patients with Cystic Fibrosis. *Antimicrob Agents Chemother*. 48: 168–171.

Sanyal, Mokaddas. 1999. The Increase in Carbapenem Use and Emergence of *Stenotrophomonas maltophilia* as an Important Nosocomial Pathogen. *J Chemother*. 11: 28–33.

Scarascia, Yap, Kaksonen, Hong. 2018. Bacteriophage Infectivity against *Pseudomonas aeruginosa* in Saline Conditions. *Front in Microbiol*. 9: 875.

Schmitz, Schuch, Fischetti. 2010. Identifying Active Phage Lysins through Functional Viral Metagenomics. *Appl Environ Microbiol*. 76: 7181–7187.

Schneider, Rasband, Eliceiri. 2012. NIH Image to ImageJ: 25 years of Image Analysis. *Nat Methods*. 9: 671-675.

Schwartz. 1976. The Adsorption of Coliphage Lambda to its Host: Effect of Variations in the Surface Density of Receptor and in Phage-receptor Affinity. *J Molec Biol*. 103: 521-536.

Sefcick, Tait, Wood. 1999. *Stenotrophomonas maltophilia*: An Increasing Problem in Patients with Acute Leukaemia. *Leuk Lymphoma*. 35: 207–211.

Shao, Wang. 2008. Bacteriophage Adsorption Rate and Optimal Lysis Time. *Genetics*. 180; 1: 471-482.

Sharahi, Azimi, Shariati, Safari, Tehrani, Hashemi. 2019. Advanced Strategies for Combating Bacterial Biofilms. *J Cell Physiol*. 234: 14689–708.

Shrivastava, Shrivastava, P., Ramasamy. 2017. World health organization releases global priority list of antibiotic-resistant bacteria to guide research, discovery, and development of new antibiotics. *J Med Soc.* 32: 76–77.

Sköld. 2001. Resistance to Trimethoprim and Sulfonamides. *Vet Res*. 32: 261-273.

Solano, Echeverz, Lasa. 2014. Biofilm Dispersion and Quorum Sensing. *Curr Opin Microbiol*. 18: 96-104.

Srichaisupakit, Chopjitt, Kerdsin. 2021. Characterization of N4-like *Pseudomonas* Phage vB_Pae-PA14 Isolated from Seawater Sampled in Thailand. *J Pure Appl Microbiol.* 15: 2347-2357.

Steinmann, Mamat, Abda, Kirchhoff, Streit, Schaible, Niemann, Kohl. 2018. Analysis of Phylogenetic Variation of *Stenotrophomonas maltophilia* Reveals Human-Specific Branches. *Front in Microbiol*. 9: 806.

Stewart. 2003. Diffusion in Biofilms. *J Bacteriol*. 185: 1485–1491.

Storms, Arsenault, Sauvageau, Cooper. 2010. Bacteriophage Adsorption Efficiency and its Effect on Amplification. *Bioprocess Biosyst Eng*. 33: 823-831.

Tkhilaishvili, Winkler, Müller, Perka, Trampuz. 2019. Bacteriophages as Adjuvant to Antibiotics for the Treatment of Periprosthetic Joint Infection Caused by Multidrug-Resistant *Pseudomonas aeruginosa*. *Antimicrob Agents Chemother*. 64: e00924-19.

Toleman, Bennett, Bennett, D., Jones, Walsh. 2007. Global Emergence of Trimethoprim/sulfamethoxazole Resistance in *Stenotrophomonas maltophilia* Mediated by Acquisition of *sul* Genes. *Emerg Infect Dis*. 13: 559–565.

Toleman, Bennett, Walsh. 2006. ISCR elements: Novel Gene-capturing Systems of the 21st Century? *Microbiol Mol Biol Rev*. 70: 296-316.

Traub, Leonhard, Bauer. 1998. *Stenotrophomonas* (*Xanthomonas*) *maltophilia*: *In vitro* Susceptibility to Selected Antimicrobial Drugs, Single and Combined, with or without Defibrinated Human Blood. J *Chemother*. 44: 293–304.

Vartivarian, Papadakis, Palacios, Manning, Anaissie. 1994. Mucocutaneous and Soft Tissue Infections Caused by *Xanthomonas maltophilia*. *Ann Intern Med*. 121: 969–973.

Valdezate, Vindel, Loza, Baquero, Cantón. 2001. Antimicrobial Susceptibilities of Unique *Stenotrophomonas maltophilia* Clinical strains. *Antimicrob Agents Chemother*. 45: 1581–1584.

Valenza, Tappe, Turnwald, Frosch, König, Hebestreit, Abele-Horn. 2008. Prevalence and Antimicrobial Susceptibility of Microorganisms Isolated from Sputa of Patients with Cystic Fibrosis. *J Cyst Fibros*. 7: 123–127.

Verma, Harjai, Chhibber. 2010. Structural Changes Induced by a Lytic Bacteriophage Make Ciprofloxacin Effective against Older Biofilm of *Klebsiella pneumoniae*. *Biofouling*. 26: 729–737.

Vicary, Newkirk, Moreland, Gonzalez, Liu, Ramsey, Leavitt. Complete Genome Sequence of *Stenotrophomonas maltophilia* Myophage Moby. *Microbiol Resour Announc*. 9: e01422-19.

Victor, Arpi, Bruun, Jønsson, Hansen. 1994. *Xanthomonas maltophilia* Bacteremia in Immunocompromised Hematological Patients. *Scand J Infect Dis*. 26: 163–170.

Vidigal, Dittmer, Steinmann, Buer, Rath, Steinmann, J. 2014. Adaptation of *Stenotrophomonas maltophilia* in Cystic Fibrosis: Molecular Diversity, Mutation Frequency and Antibiotic Resistance. *Int J Med Microbiol*. 304: 613–619.

Walkty, Adam, Baxter, Denisuik, Lagacé-Wiens, Karlowsky, Hoban, Zhanel. 2014. *In vitro* Activity of Plazomicin against 5,015 Gram-negative and Gram-positive Clinical Isolates Obtained from Patients in Canadian Hospitals as Part of the CANWARD Study, 2011-2012. *Antimicrob Agents Chemother*. 58: 2554–2563.

Walmagh, Boczkowska, Grymonprez, Briers, Drulis-Kawa, Lavigne. 2013. Characterization of Five Novel Endolysins from Gram-negative Infecting Bacteriophages. *Appl Microbiol Biotechnol.* 97: 4369–4375.

Wang, Scipione, Dubrovskaya, Papadopoulos. 2014. Monotherapy with Fluoroquinolone or Trimethoprim-sulfamethoxazole for Treatment of *Stenotrophomonas maltophilia* Infections. *Antimicrob Agents Chemother.* 58: 176–182.

Waters, Neill, Kaman, Sahota, Clokie, Winstanley, Kadioglu. 2017. Phage Therapy is Highly Effective against Chronic Lung Infections with *Pseudomonas aeruginosa*. 72: 666-667.

Wienhold, Lienau, Witzenrath. 2019. Towards Inhaled Phage Therapy in Western Europe. *Viruses.* 11: 295.

Wright, Hawkins, Anggård, Harper. 2009. A Controlled Clinical Trial of a Therapeutic Bacteriophage Preparation in Chronic Otitis due to Antibiotic-resistant *Pseudomonas aeruginosa*; a Preliminary Report of Efficacy. *Clin Otolaryngol*. 34: 349-357.

Wu, Wang, Shiau, Wang, Lauderdale, Chang, TSAR Hospitals. 2012. A Multicenter Surveillance of Antimicrobial Resistance on *Stenotrophomonas maltophilia* in Taiwan. *J Microbiol Immunol Infect.* 45: 120–126.

Wu, Zhang, Jiang, Wu, Sun, Huang. 2021. Characterization and Genomic Analysis of ϕSHP3, a New Transposable Bacteriophage Infecting *Stenotrophomonas maltophilia*. *J Virol.* 95: 00019-00021.

Yang, Liang, Lin, Jia. 2010. Isolation and Characterization of a Virulent Bacteriophage AB1 of *Acinetobacter baumannii*. *BMC Microbiol*. 10: 131.

Yehl, Lemire, Yang, Ando, Mimee, Torres, de la Fuente-Nunez, Lu. 2019. Engineering Phage Host-Range and Suppressing Bacterial Resistance through Phage Tail Fiber Mutagenesis. *Cell*. 179: 459–469.

Young. 2013. Phage lysis: Do We Have the Hole Story Yet? *Curr Opin Microbiol*. 16: 790–797.

Yu, Mathieu, Li, Dai, Alvarez. 2015. Isolation of Polyvalent Bacteriophages by Sequential Multiple-Host Approaches. *Appl Environ Microbiol*. 82: 808-815.

Zhanel, Adam, Baxter, Fuller, Nichol, Denisuik, Lagacé-Wiens, Walkty, Karlowsky, Schweizer, Hoban, Canadian Antimicrobial Resistance Alliance. 2013. Antimicrobial Susceptibility of 22746 Pathogens from Canadian Hospitals: Results of the CANWARD 2007-11 Study. *Antimicrob Chemother*. 68: i7–i22.

Zhang, Li, 2013. Biological Characteristics of Phage SM1 for *Stenotrophomonas maltophilia* and its Effect in Animal Infection Model. *Zhejiang Da Xue Xue Bao Yi Xue Ban*. 42: 331-336.

Zhang, Zhang, R., Hu, Liu, Wang, An, Song, Shi, Fan, Tong, Liu, H. 2021. Biological Characteristics and Genomic Analysis of a *Stenotrophomonas maltophilia* Phage vB_SmaS_BUCT548. *Virus Genes.* 57: 205–216.